## Original Study

Franco Foresta Martin*, Donatella Barca, Ivona Posedi

# Evidencing Human Occupation of a Small Island Through Ancient Glass: The Case of Ustica (Palermo, Italy)

**Abstract:** The subject of this study consists of 17 ancient glass fragments from the island of Ustica (Palermo, Italy) obtained from local museums. All the 17 glass fragments are stratigraphically decontextualized, as they were collected by archaeological surface surveys. Each fragment was analyzed by Electron Micro Probe Analyzer coupled with an Energy Dispersive X-Ray System (EMPA-EDS) and by Laser Ablation-Inductively Coupled Plasma-Mass Spectrometry (LA-ICP-MS) to obtain the composition of major, minor and trace elements. Surface analyses revealed the presence of corrosion layers in most of the glass fragments which was evident also in the chemical data. Nevertheless, reconstruction of the glassmaking processes and the approximate period of production was possible for almost all the glass fragments. Less than half of the examined fragments are attributable to recognizable typologies as unguentaria, beakers, bottles, and vases; all the other small fragments are typologically undetermined. Out of 17 fragments only one fragment is of HLLA composition possibly being produced in 17th–18th century AD, while all the others can be attributed to soda glass with different periods of production: natron glass from Roman and Early Medieval period, plant-ash glass from High or Late Medieval period with the exception of possible Byzantine glass from 6th century AD, and synthetic soda glasses typical of modern era. These data confirm the discontinuous habitation of the island from the Roman period as well as the import of glass objects to the island.

**Keywords:** Ancient glass, Roman glass, Medieval glass, Ustica island, Archaeovitreology

## 1 Introduction

This work provides the first archaeometric study of ancient glass fragments found in Ustica. Ustica is a small Italian island located ca. 70 km northwest of Sicilian coast (Figure 1) reported by geologists as a case study of hot spot volcanism in the Southern Tyrrhenian Sea (Foresta Martin, 2014).

Ustica has been discontinuously inhabited since prehistoric times and it has rich archaeological heritage consisting of ruins of ancient settlements and abundant ceramic finds (Spatafora & Mannino, 2008; Mannino & Ailara, 2016).

*Corresponding author: Franco Foresta Martin**, Laboratorio Museo di Scienze della Terra Isola di Ustica, Palermo, Italy; Istituto Nazionale di Geofisica e Vulcanologia, Sezione di Palermo, Italy, E-mail: sidereus@rocketmail.com
**Donatella Barca,** Università della Calabria, Arcavacata di Rende, Cosenza, Italy
**Ivona Posedi,** University of Lincoln, College of Arts, School of History and Heritage, Lincoln, UK
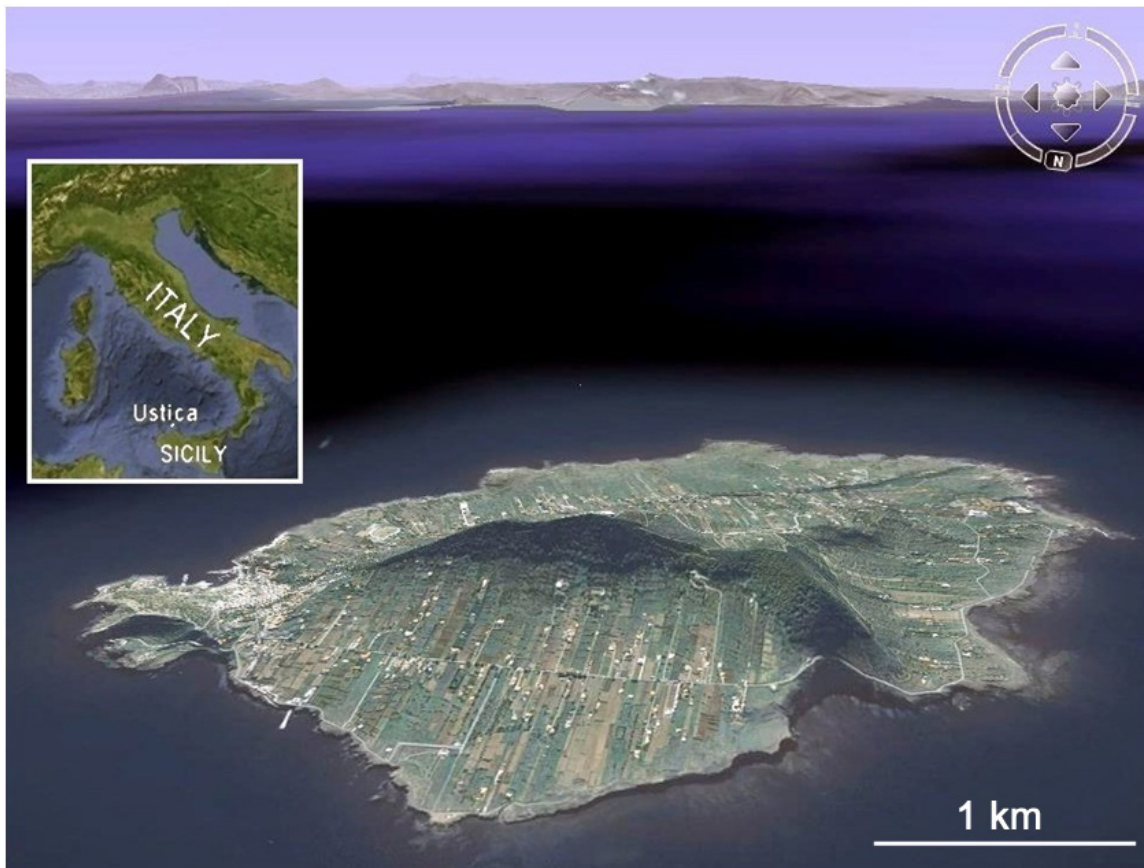
**Figure 1:** The island of Ustica and the north-western coast of Sicily visible on the horizon. From Google Earth.

On the island of Ustica, there is no evidence of ancient glass-making. The few preserved glass fragments kept in the local museums are probably part of artifacts imported from the mainland in ancient times and they have not been taken into consideration for any Archaeovitreological[1] study until now.

The fragments analyzed in this study come from two different contexts: a group of 13 pieces (USPAR from 1 to 13, Figure 2a) belongs to the S. Ferdinando Re Parish Museum of Ustica which preserves, among other things, obsidians and ceramic finds from different prehistoric and historic epochs; another group of 4 fragments (USTRA from 1 to 4, Figure 2b) belongs to the collection of Laboratorio Museo di Scienze della Terra, and they were collected on the surface of an agricultural field in the Tramontana Sopravia district of Ustica where archaeologists reported evidence of late Roman ceramics (Spatafora & Mannino, 2008; Mannino & Ailara, 2016).

Both assemblages contain glass fragments that are not easily typologically classified; furthermore, the lack of the stratigraphic context prevents the determination of their dating.

The objectives of this work are:
–    the attribution of each fragment to a specific object, where possible;
–    the characterization of the raw materials used in the production of these glass fragments;
–    the formulation of a hypothetical dating of these glass finds.

---

[1]  Archaeovitreology as used by Posedi, Kertész, Barrulas, Fronza, Schiavon and Mirão, 2019.
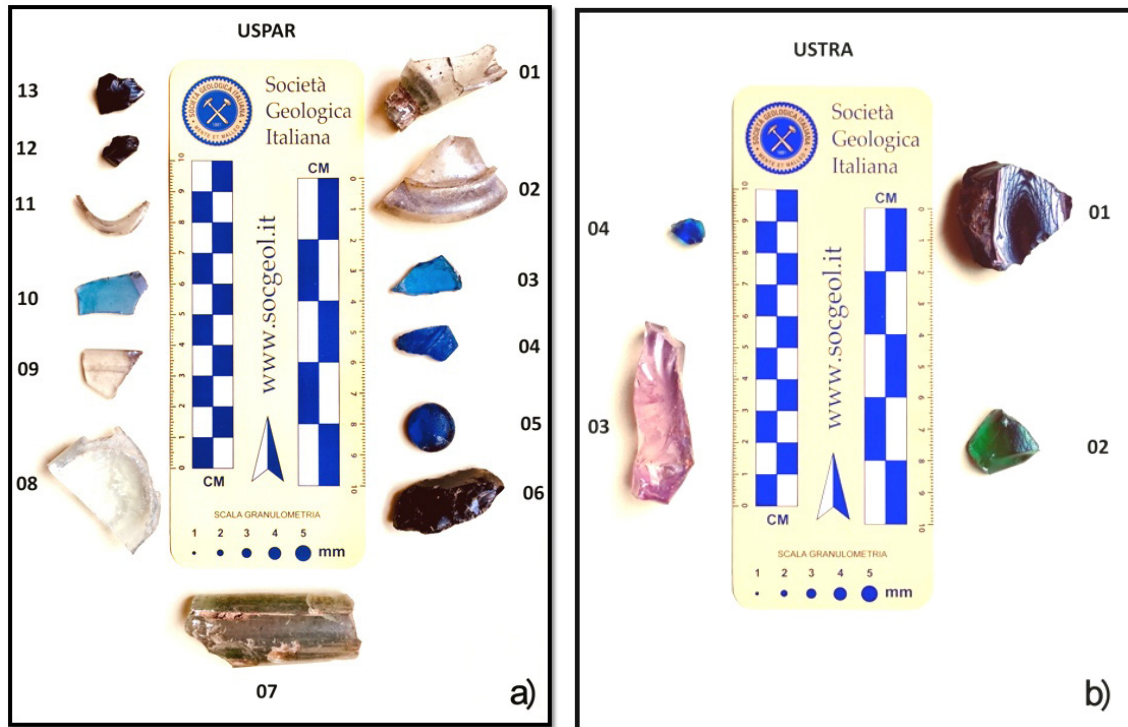
**Figure 2:** The two assemblages of glass fragments examined in this study: **a)** USPAR-01-13; **b)** USTRA-01-04.

# 2 Background on the Ancient Glassmaking

Nowadays we know that the typical ancient glass recipe requires mixing three fundamental components which are heated up to their melting point: a silica-based vitrifying agent ($SiO_2$) as the lattice former; a flux based on alkaline and alkaline earth compounds ($Na_2O$, $K_2O$, $MgO$) to lower the high melting temperature of silica (around 1700°C); and a stabilizer such as calcium oxide ($CaO$) to slow down the processes of glass alteration over time (e.g., Freestone, 2005; Gratuze & Janssens, 2004; Wedepohl, Simon, & Kronz, 2011; and references therein) (Figure 3). In short, glass is made of a silica-alkali-lime mixture that chemically behaves as a eutectic whose melting point is lower (below 1000°C) than that of the individual components (Degryse, Scott & Brems, 2014). During the multi-millennial history of glass, these three basic components have always remained the same although their relative abundances in the recipes adopted and the raw materials used have changed.
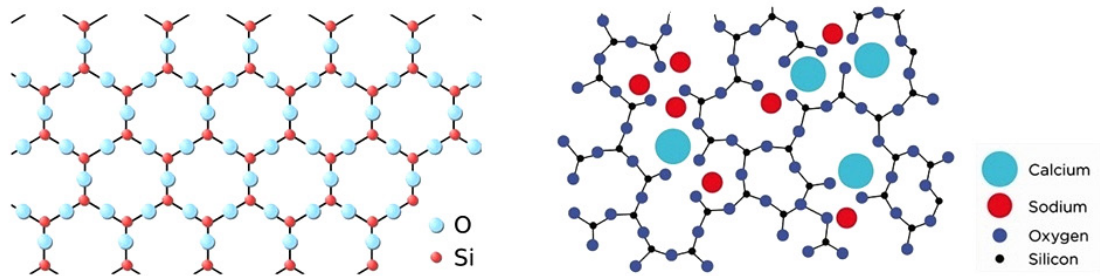


**Figure 3:** The ordered crystal lattice of silica (left) typical of minerals, and random lattice (right) typical of glass, with the addition of fluxes (sodium) and stabilizers (calcium). From the public domain.

Legend tells that the first glass was made accidentally in ancient Phoenicia by exposing the glass ingredients to fire. After this fortuitous discovery, human intelligence would have perfected glass processing in an empirical way, by trial and error, as reported by Pliny the Elder in Natural History (XXXI, 107 and XXXVI, 193–4, English edition edited by Rackham & Jones, 1962).

Recent studies have ascertained that the processing of artificial glass is much older than was believed and that it began in the Bronze Age or just before it (Gratuze & Janssens, 2004). The analyses on vitreous finds from various epochs have made it possible to know which raw materials were used in antiquity and what is their provenance (Rehren & Freestone, 2015). It was thus possible to reconstruct, in broad terms, the technological evolution of glass production over the millennia (Wedepohl, Simon, & Kronz, 2011) (Figure 4).

The first artifacts covered with vitrified surfaces such as glazed quartz and faience appeared in Mesopotamia in the 4th millennium BC (Early Bronze Age) and then spread in Phoenicia and Egypt (Tite, Shortland & Painter, 2002). Around 1600 BC (Middle Bronze Age) the production of ornamental glass objects such as colorful beads and amulets began in Mesopotamia and other regions of the Near East (Gratuze, 2013; Angelini, Gratuze, & Artioli, 2019; and references therein). These artifacts were obtained by melting coastal sands rich in quartz granules and in carbonate shells together with ash from plants containing alkalis as flux; hence the definition of plant-ash glass (Freestone, Hughes, & Stapleton, 2008; Wedepohl, 2011; Gratuze, 2013). A distinctive feature of plant-ash glasses is the relative abundance of potassium and magnesium ($K_2O$ and $MgO$, each > 1.5% by weight), which derives from the richness of these elements in the halophytic plants used to obtain ash (Sayre & Smith, 1961; Janssens, 2013).
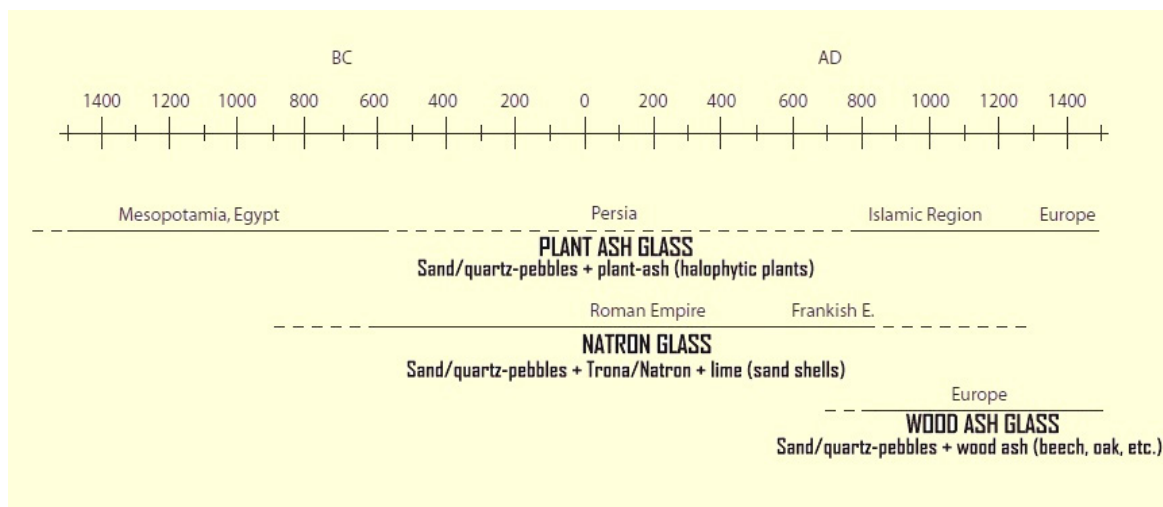


**Figure 4:** Chronological scheme of the various types of glass produced in antiquity. Modified from Wedepohl et al. (2011).

Starting from the middle of the 1st millennium BC, the Near East regions adopted another recipe for the production of glass in which the plant-ash was replaced with a mineral salt flux consisting of *trona* or *natron*[2]. *These* sodium carbonates are found in some evaporitic basins like those of the Wadi El Natrun valley in Egypt (Freestone et al., 2008). The natron glass had spread from the Near East to Europe and Asia where it becomes dominant until the 9th century AD. Natron glass is generically called Roman glass even if found in contexts that precede or succeed the period of the Roman Empire (Freestone et al., 2008; Wedepohl et al., 2011; Gratuze, 2013). Since trona and natron are poor in potassium and magnesium, Roman glass can be distinguished from plant-ash glass by $K_2O$ and $MgO$ <1.5 wt% (Sayre & Smith, 1961). Most of the Roman glass groups are chemically homogeneous throughout the Empire within some variability in major elements (Degryse, 2014), comparing to wood-ash glasses (Table 1).

---

**2** From the chemical point of view, *trona* is trisodium hydrogendicarbonate dihydrate $Na_3(CO_3)(HCO_3) \cdot 2(H_2O)$; *natron* is sodium carbonate decahydrate $Na_2CO_3 \cdot 10H_2O$.

**Table 1:** Average values and compositional intervals of the major elements (in wt%) in the Roman glass of the first millennium AD, produced in the eastern and western part of the Roman Empire. From Degryse (2014).

|  | Mean | StDev | Lower limit | Upper limit |
|---|---|---|---|---|
| $SiO_2$ | 69.54 | 2.53 | 64.48 | 74.60 |
| $Na_2O$ | 16.63 | 1.50 | 13.63 | 19.63 |
| $K_2O$ | 0.75 | 0.24 | 0.27 | 1.23 |
| $CaO$ | 7.48 | 1.18 | 5.12 | 9.84 |
| $MgO$ | 0.59 | 0.29 | 0.01 | 1.17 |
| $Fe_2O_3$ | 0.62 | 0.48 | 0.00 | 1.58 |
| $Al_2O_3$ | 2.59 | 0.38 | 1.83 | 3.35 |
| $P_2O_5$ | 0.12 | 0.05 | 0.02 | 0.22 |
| $MnO$ | 0.73 | 0.74 | 0.00 | 2.21 |
| $TiO_2$ | 0.13 | 0.14 | 0.00 | 0.41 |

Two different models of production and distribution of glass in the Roman period are debated nowadays. One model describes the existence of primary workshops in the Near East (Egypt, Israel, Palestine, Syria) where the raw glass was produced locally and then exported in big ingots to a large number of secondary glass-working centers scattered in the various parts of the Empire. There, the ingots were recast and made into finished products (Freestone, 2005). This model would explain why distant locations have glasses with the identical chemical composition which is attributable to some specific areas of sand and natron supply and can be associated with primary workshops, as confirmed by archaeological discoveries (Nenna, 2015; Picon & Vichy, 2003).

In the literature some compositional groups are indicated with explicit reference to the place of origin of the raw materials such as Wadi Natrun or Egypt I, Egypt II, Levantine I, Levantine II; others with reference to chemical characteristics such as HIMT for glasses with percentages of iron, magnesium, and titanium higher than typical Roman glass (Freestone, 2001 and references therein; Freestone, Wolf, & Thirlwall, 2009), (Table 2 and Figure 5).

**Table 2:** Some of the most widespread compositional groups of Roman Glass characterized by the use of natron as flux, produced in the 1st millennium AD from raw materials extracted in the Near East. Data from literature (Sayre & Smith, 1961; Gratuze & Barrandon, 1990; Mirti, Casoli, & Appollonia, 1993; Freestone, Gorin-Rosen, & Hughes, 2000; Nenna, 2000; Freestone et al., 2008; and references therein).

| COMPOSITIONAL GROUPS | LOCALITY | RAW MATERIALS | CHEMICAL COMPOSITION | PERIOD OF PRODUCTION |
|---|---|---|---|---|
| Wadi Natrun or Egypt I | Egypt | Egyptian sand and natron | $Al_2O_3$~3–4.5 wt% $CaO$~3–4 wt% | VII–VIII Century AD |
| Egypt II | Egypt | Egyptian sand and natron | $Al_2O_3$~1.5–2.5 wt% $CaO$~9–10 wt% | VIII–IX Century AD |
| Levantine I | Israel, Palestine | Sand of Belus River and natron | $Al_2O_3$~3 wt% $CaO$~8 wt% | IV–VIII Century AD |
| Levantine II | Israel | Coastal sand and natron | $Al_2O_3$~3 wt% $CaO$~7 wt% | VI–VII Century AD |
| European-Roman | Roman Europe | Coastal sand and natron | $Al_2O_3$~2–2.5 wt% $CaO$~4–6 wt% | I–VI Century AD |
| HIMT | Egypt | Sand of Nilo River mouth and natron of Mount Sinai | $Al_2O_3$~3 wt% $CaO$~5 wt% High Fe, Mn, and Ti | IV–VIII Century AD |
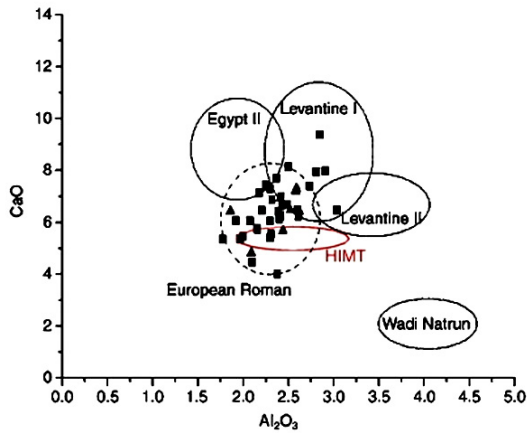
**Figure 5:** Binary graph Al$_2$O$_3$ vs CaO which discriminates some of the compositional groups of Roman glass. Modified from Arletti, Vezzalini, Biaggio Simona, & Maselli Scotti (2008).

According to another model of production and distribution, the compositional homogeneity of the Roman glass would be due to the diffusion of a successful recipe made with local sands and imported natron from the Near East (Arletti et al., 2008). The experimental research on the coastal sands of the Western Mediterranean (Archglass Project) has verified that in this part of the Basin the coastal sands suitable for producing good quality Roman glass exists, even if they are rare. Three of these coastal sands have been found in Italy: in Basilicata, between the mouths of Basento and Bradano rivers; in Puglia, southeast of Brindisi; and in Tuscany, between Piombino and Follonica. Two are found in Spain: river mouth of the Rio Guadiana, and the coast of the city of Aguilas. One is in France at Hière Bay (Degryse, 2004; Brems, Degryse, Hasendoncks, Gimeno, Silvestri, Vassilieva, Luypaers, & Honings, 2012).

Due to probable exhaustion of natron sources in the Near East at the end of the 1st millennium AD, the plant-ash flux made a come-back in both the Islamic world and in Mediterranean Europe, while the rest of Europe used wood-ash flux which is poor in sodium (<6 wt%) and rich in potassium (Wedepohl et al., 2011). Two sub-types of wood-ash glass are distinguished depending on the potassium to calcium ratio (K$_2$O:CaO): the *forest* glass has K$_2$O:CaO >0.5, while high lime-low alkali (HLLA) glass has K$_2$O:CaO <0.5 (Schalm, Janssens, Wouters, & Caluwé, 2007).

Recycling is a factor that makes the compositional diagnosis, in terms of glass provenance, complex: it was adopted on a large scale as early as the Roman Imperial Era, as confirmed by loads of glass scrap found and recovered from the wrecks of ancient Roman ships (Auriemma, 2000; Toniolo, 2005).

# 3  Study Area

The island of Ustica (Figure 1), located 70 km north of the coast of Palermo (Sicily, Italy), is a small sub-aerial part of a large submarine volcanic complex that rises over 2200 m from the bottom of the Tyrrhenian Sea. The volcanic activity was both submarine (starting ~1 Ma) and sub-aerial (500 ka–130 ka) and is now considered extinct. The eruptive products range in composition from basalts to trachyte (Na-alkaline affinity). Despite the observed degree of magmas evolution, no obsidian rocks have been reported in the deposits of this volcanic island (de Vita, Laurenzi, Orsi, & Voltaggio, 1998; Foresta Martin, 2014; de Vita & Foresta Martin, 2017).

The island of Ustica is the northernmost prehistoric settlement of the western Sicily region and a center of ancient trade and cultural exchanges. The island has been inhabited since the introduction of the agriculture in the Central Mediterranean, as demonstrated by the Neolithic settlement of Spalmatore (6th–5th millennium BC), the Eneolithic settlement of Piano dei Cardoni (4th–3rd millennium BC), the Early Bronze Age village of Colunnella (3rd–2nd millennium BC) and the Middle Bronze Age village of Faraglioni

(14th–13th century BC). A single Mycenean type of glass bead was found during an archaeological excavation in the Faraglioni Village (Spatafora & Mannino, 2008; Mannino & Ailara, 2016). The aforementioned archaeological sites exhibit a lot of ceramic finds and are also rich in obsidian fragments which mainly derive as imports from Lipari and Pantelleria (Tykot, 1995; Foresta Martin, Di Piazza, D'Oriano, Carapezza, Paonita, Rotolo, & Sagnotti, 2017; Foresta Martin & La Monica, 2019).

After a sudden and still unexplained abandonment of the Faraglioni Middle Bronze Age Village around 1200 BC the island remained uninhabited for many centuries. Between the 4th and 3rd centuries BC, during the Hellenistic-Roman age, there is evidence of the re-colonization of the island. A big settlement with a nearby necropolis flourished on the Rocca della Falconiera, the top of an extinct tuff cone-volcano, 157 m amsl on the east side of the island. The choice of that isolated position, exposed to winds and bad weather, must have been prompted by defensive needs and by the possibility of controlling the main natural harbor of the island, Cala S. Maria (Spatafora & Mannino, 2008; Mannino & Ailara, 2016). A lot of archaeological material has been recovered on the Rocca della Falconiera. The most significant finds are ceramic table vases and transport vases, most of which are dated between the 3rd and the 1st centuries BC; bronze necklaces and coins; and a single glass object, an undamaged balsamarium now exposed in the *Museo Civico Archeologico P.C. Seminara* of Ustica (Spatafora & Mannino, 2008; Mannino & Ailara, 2016).

A few centuries later, in the late-Roman and Byzantine Age, it seems that a more widespread occupation of the island has occurred, as evidenced by the ruins of villages and by the abundance of ceramic finds dating from the 5th to the 6th century AD, scattered in the Petriera, Tramontana, and Spalmatore areas (Spatafora & Mannino, 2008; Mannino & Ailara, 2016). A large paleo-Christian necropolis located on the south and western slopes of Falconiera belongs to this period and it includes several hypogean graves. Some precious funerary objects, taken from these tombs during excavations carried out at the end of the 1700s, were donated to the Bourbon monarchs and then they were lost; some others are visible in the showcases of the "Museo Civico Archeologico P.C. Seminara" of Ustica (Spatafora & Mannino, 2008; Mannino & Ailara, 2016).

Around the 7th and 8th centuries AD the political instability of Sicily and the insecurity of the maritime routes, often exposed to the assault of the corsairs, caused a decrease in the population of Ustica. The island remained deserted for about four centuries until the second half of the 1200s when the Normans decided to establish a Benedictine monastery on Case Vecchie village accompanied by a small agro-pastoral community. The settlement survived for about two centuries until the second half of the 15th century AD when the island of Ustica was occupied by the North African corsairs who transformed it into a base to launch their incursions along the maritime routes between Sicily and the continent. The last colonization of the island of Ustica, from which the current population descends, was promoted by the Bourbons in the second half of the 1700s, in order to remove the domination of the North African corsairs from the island (Ailara, 2015).

It is remarkable that of all the ancient human settlements described in this rapid excursus – the prehistoric, the Roman and the Medieval ones – there is archaeological evidence in the form of ceramic finds, but rarely as glass artifacts. In addition to the two glass artifacts previously mentioned (the Mycenaean bead and the Roman balsamarium), some other historical glasses can be found scattered in agricultural fields. These fragments are, at first glance, not visually recognizable nor diagnosable and can be mixed with modern glass debris.
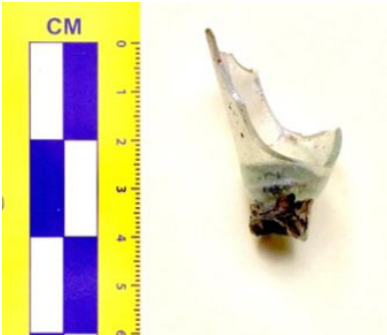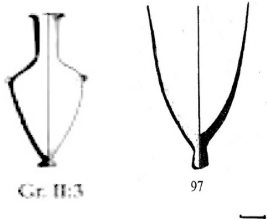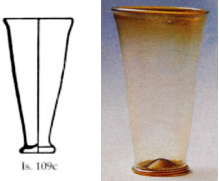
## 4 Materials and Methods

The 17 glass fragments of Ustica assemblage were first subjected to typological classification where possible. This has been followed by geochemical glass analyses to establish the chemical composition, attempting to identify the period of production.
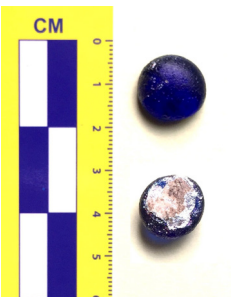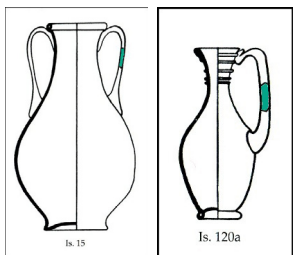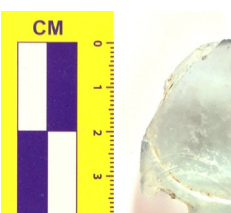
## 4.1 Samples

In the present study, 17 glass finds have been analyzed which can be subdivided into two groups. The first group includes 13 pieces (USPAR from 01 to 13, Figure 2a) that belong to the *S. Ferdinando Re Parish Museum* of Ustica; they lack indications concerning the archaeological context in which were collected. The second group of 4 fragments (USTRA from 01 to 04, Figure 2b) was collected in the Tramontana Sopravia district of Ustica where there is archaeological evidence of late Roman settlements dating from the 4th to the 6th century AD (Spatafora & Mannino, 2008; Mannino & Ailara, 2016).

Because of the fragmentation of glass finds, some of them lack diagnostic elements that would allow their attribution. Therefore, only 8 glass fragments can be classified as being parts of various containers (vases, amphorae, beakers) or decorations (Table 3).

**Table 3:** Typological analyses (N.I. = Non Identified).

| SAMPLE | DESCRIPTION | POSSIBLE TYPE |
|---|---|---|
| USPAR-01  | Fragment of the bottom of a conic-truncated container. Colorless, with many impurities and bubbles. There are traces of silver-colored paint on the exterior wall. | Unguentarium, Isings (1957) Gr. II:3; Oil Lamp with a pointed base, 97, after Križanac, 2016.  |
| USPAR-02  | Fragment of the bottom of a beaker with a ringed base. Colorless with many impurities, millimetric bubbles, and iridescence. | Beaker, compatible with the form Isings (1957), 109c. I.e.: beaker from S.Agata Necropolis, 5th C. AD, Himera Antiquarium, Palermo (Basile, Carreras Rossell, Greco & Spanò Giammellaro, 2004).  |
| USPAR-03  | Fragment of a wall of a container. Color: blue. | N.I. |
| USPAR-04  | Fragment of a rim of a container decorated with a rib on the exterior wall. Color: dark blue. | Compatible with a beaker or a cup. |

| SAMPLE | DESCRIPTION | POSSIBLE TYPE |
|---|---|---|
| USPAR-05 | Small disk with the shape of a plane-convex lens (superior face convex, inferior face plate). Color: dark blue. Trace of white glue in the inferior face. | Similar to Gaming Piece Isings (1957) Ch. n. 32. But much more probably it was a decorative element attached to the walls of a bottle, as in the 3d -4th C. bottle, Museo Archeologico Ibleo, Ragusa (Basile et al., 2004). |
| USPAR-06 | Fragment of the wall of a thick (1 cm) container. Color: black in reflected light; brown in transmitted light. | N.I. |
| USPAR-07 | Fragment of a thick listel with a plane-convex section. Color: green. Many impurities and bubbles. | Handle of an amphora or of a hewer, as forms Isings (1957) 15 or 120a. |
| USPAR-08 | Fragment of the bottom of a container with semi-circular shape. A stamp is visible that might represent number 3. It is probably a manufacturer code or the measure of the container capacity. Colorless. | Compatible with the bottom of a modern bottle. |
| USPAR-09 | Fragment of a rim of a container with lip everted and grooved on inside wall. Colorless. | Compatible with a cup or a beaker. I.e.: Isings (1957) 2, 33 or 86. |
| USPAR-10 | Fragment of a wall of a container. Color: blue. | N.I. |

| SAMPLE | DESCRIPTION | POSSIBLE TYPE |
|---|---|---|
| USPAR-11 | Small sickle-shaped fragment that fits perfectly with the wall of USPAR 01. Colorless. | (See USPAR 01) |
| USPAR-12 | Small shapeless fragment. Color: purple. | N.I. |
| USPAR-13 | Small shapeless fragment. Color: purple. | N.I. |
| USTRA-01 | Thick (1 cm) fragment of the wall of a container. Color: black in reflected light; dark green/brown in transmitted light. | N.I. |
| USTRA-02 | Thick (1 cm) fragment of the wall of a container. Color: green. | N.I. |
| USTRA-03 | Thick (1 cm) fragment of the wall of a container with an ornamental pattern in relief. Color: pink. | N.I. |
| USTRA-04 | Small shapeless fragment. Color: blue. | N.I: |
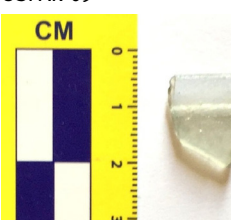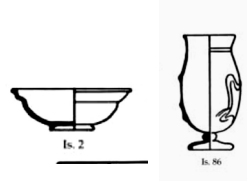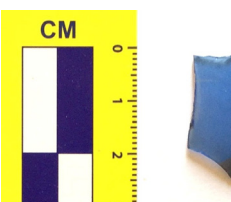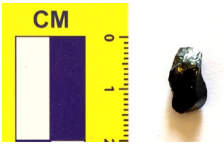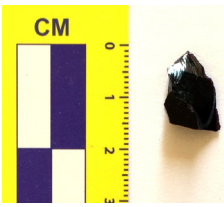
## 4.2 Experimental

Geochemical studies were performed at the Department of Biology, Ecology and Earth Sciences, University of Calabria (Italy) by means of two different analytical methods: EPMA-EDS (Electron Probe Micro Analyzer coupled with Energy-Dispersive X-ray Spectrometry) for the determination of major and minor elements in wt%, and LA-ICP-MS (Laser Ablation - Inductively Coupled Plasma - Mass Spectrometry) for the determination of trace element concentrations in ppm (Barca, De Francesco, Crisci & Tozzi, 2008; Barca, Abate, Crisci, & De Presbiteris, 2009). Before the analyses, a small fragment (about 3x3 mm) was detached with tweezers from each sample, then fixed on a slide, and its surface was covered by a carbon sputter coating.

EPMA-EDS analyses were carried out using a JEOL-JXA 8230, equipped with an EDS - JEOL EX-94310FaL1Q spectrometer under the following operating conditions for chemical analyses: acceleration voltage 15kV, probe current 10 nA, probe diameter 10 µm, standardless quantification was performed using a Quant Correction ZAF. Furthermore, to avoid the loss of Na and ensure the correct acquisition of other element concentrations, an acquisition time of 15 sec was selected. Three-point analyses were carried out on each glass fragment. The detection limits for most elements were about 0.2 wt%.

LA-ICP-MS analyses were carried out using an Elan DRCe instrument (Perkin Elmer/SCIEX), connected to a New Wave UP213 Nd-YAG laser probe (213 nm). The samples were ablated by a laser beam in a cell under a moderate flow of pure helium. Then, behind the cell, the ablated material was flushed in a continuous flow of a helium and argon mixture to the ICP system where it was atomized and ionized for quantification in the mass spectrometer (Gunther & Heinrich, 1999).

Ablation was performed with spots of 50 microns with a constant laser repetition rate of 10 Hz and fluence of about 20 Jcm$^{-2}$ (Barca et al., 2008, 2009).

In detail, for each analysis, after 5 s of pre-ablation, a transient signal of intensity versus time was obtained for each element using a 60 s background level (acquisition of gas blanks) followed by 40 s of ablation and then 60 s of post-ablation at background levels. Data were transmitted to a PC and processed by the Glitter program (van Achterberg, Ryan, Jackson, & Griffin, 2001). Three-point analyses were carried out on each glass fragment. The detection limits for most elements were approximately 0.01 ppm.

Calibration was performed on glass reference material SRM 612–50 ppm by NIST in conjunction with internal standardization, applying $SiO_2$ concentrations from EPMA-EDS analyses (Fryer, Jackson, & Longerich, 1995).

In order to evaluate possible errors within each analytical sequence, determinations were also made on the SRM 610–500 ppm by NIST and on BCR 2G by USGS glass reference materials as unknown samples and element concentrations were compared with reference values from the literature (Pearce, Perkins, Westgate, Gorton, Jackson, Neal, & Chenery, 1997; Gao et al., 2002). The accuracy (i.e. the relative difference from reference values) was generally better than 12% and most elements plotted in the range +/− 8% (Table 4).

EPMA-EDS and LA-ICP-MS analyses were carried out for all samples except USPRA 06, for which only the analysis of the major elements with EPMA-EDS was made.

# 5 Results and Discussion

EMPA-EDS is a surface analysis technique with a penetration depth of approximately 1 µm (Lifshin, 2006). This implies that when the degraded glass layer is very thin and not noticeable upon a macroscopic inspection, the analyses performed with EMPA-EDS (major and minor elements) do not reflect the original composition of the pristine glass but that of the altered surface. The Ustica glass fragments did not display significant visual signs of surface deterioration which tends to be a characteristic of soda glass as they are less prone to heavy deterioration than potassium-based (wood-ash) glasses (Orlando, Olmi, Vaggelli, & Bacci, 1996; Ortega-Feliu, Gómez-Tubío, Respaldiza, & Capel, 2011; De Bardi, Wiesinger, & Schreiner, 2013). The lack of degradation or its minimal impact (heterogeneity in occurrence and thickness) on soda glasses coming from archaeological contexts has been noted in previous studies (Genga, Siciliano, Famà, Filippo, Siciliano, Mangone, Traini, & Laganara, 2008; Posedi, 2016; Posedi, Kertész, Barrulas, Fronza, Schiavon, &

**Table 4:** Analyses by LA-ICP-MS of BCR-2G and NIST SRM 610 standard glass (in ppm); StDev=standard deviation. Comparison between literature data (Gao et al., 2002) and results from the present study.

| | BCR-2G | | | | | NIST-SRM610 | | | | |
| | Gao et al. (2002) | | This study[1] | | Accuracies[2] | Gao et al. (2002) | | This study[1] | | Accuracies[2] |
| | Concentrations | StDev | Concentrations | StDev | | Concentrations | StDev | Concentrations | StDev | |
|---|---|---|---|---|---|---|---|---|---|---|
| Ti | 13005 | 1081 | 13953 | 525 | -7.3 | 434 | 9 | 422 | 13 | -2.76 |
| V | 425 | 7 | 448 | 10.4 | -5.46 | 442 | 5 | 426 | 8 | 3.62 |
| Cr | 17 | 2 | 16.1 | 0.8 | 5.06 | 404 | 7 | 418 | 6 | -3.47 |
| Co | 38 | 1 | 40.2 | 2.1 | -5.79 | 405 | 5 | 415 | 8 | -2.47 |
| Cu | 18 | 1 | 19.5 | 1.2 | -8.83 | 430 | 11 | 441 | 10 | -2.56 |
| Ni | 12.7 | 0.9 | 12.2 | 0.7 | 3.94 | 445 | 12 | 436 | 11 | 2.02 |
| Zn | 153 | 9 | 163 | 13.6 | -6.54 | 455 | 20 | 467 | 16 | -2.64 |
| As | - | - | - | - | - | - | - | 362 | 11 | - |
| Rb | 51 | 3 | 48.5 | 3.6 | 5.08 | 431 | 6 | 441 | 18 | -2.32 |
| Sr | 321 | 6 | 336 | 9 | -4.76 | 497 | 5 | 478 | 7 | 3.82 |
| Y | 31 | 2 | 33 | 1.7 | -7.32 | 450 | 7 | 433 | 10 | 3.78 |
| Zr | 167 | 8 | 158 | 6.4 | 5.56 | 439 | 7 | 447 | 12 | -1.82 |
| Nb | 10.9 | 0.6 | 12 | 0.9 | -10.1 | 420 | 5 | 429 | 6 | -2.14 |
| Sn | 2.4 | 0.4 | 2.5 | 0.2 | -4.17 | 400 | 10 | 412 | 8 | -3.00 |
| Sb | 0.51 | 0.87 | 0.53 | 0.04 | -3.92 | 377 | 27 | 406 | 12 | -7.69 |
| Ba | 641 | 14 | 656 | 13 | -2.41 | 425 | 6 | 435 | 13 | -2.35 |
| Pb | 10.9 | 0.5 | 11.6 | 1.13 | -6.42 | 413 | 7 | 427 | 16 | -3.39 |
| La | 25 | 1 | 24.4 | 2 | 2.56 | 457 | 6 | 448 | 8 | 1.97 |
| Ce | 52 | 2 | 55.9 | 2 | -7.52 | 448 | 6 | 439 | 7 | 2.01 |
| Pr | 6.3 | 0.4 | 7.0 | 0.5 | -11.1 | 430 | 5 | 436 | 7 | -1.40 |
| Nd | 27 | 1 | 28.3 | 1.2 | -4.81 | 430 | 5 | 443 | 8 | -3.02 |
| Sm | 6.3 | 0.5 | 6.7 | 0.3 | -6.35 | 449 | 10 | 456 | 11 | -1.56 |
| Eu | 1.91 | 0.09 | 2.1 | 0.1 | -9.95 | 460 | 5 | 442 | 6 | 3.91 |
| Gd | 6.5 | 0.6 | 5.9 | 0.5 | 9.23 | 420 | 6 | 413 | 8 | 1.67 |
| Tb | 0.95 | 0.07 | 0.87 | 0.08 | 8.0 | 442 | 6 | 432 | 8 | 2.26 |
| Dy | 6.0 | 0.4 | 5.42 | 0.6 | 9.67 | 426 | 7 | 437 | 7 | -2.58 |
| Ho | 1.2 | 0.07 | 1.06 | 0.04 | 11.67 | 448 | 8 | 438 | 10 | 2.23 |
| Er | 3.3 | 0.2 | 3.49 | 0.3 | -5.76 | 426 | 7 | 423 | 7 | 0.70 |
| Tm | 0.46 | 0.04 | 0.49 | 0.05 | -6.52 | 420 | 8 | 439 | 8 | -4.52 |
| Yb | 3.2 | 0.3 | 2.95 | 0.4 | 7.81 | 460 | 9 | 448 | 11 | 2.61 |
| Lu | 0.47 | 0.04 | 0.44 | 0.05 | 7.02 | 435 | 9 | 422 | 9 | 2.99 |

(1) Values determined by LA-ICP-MS. Mean values of 10 determinations.
(2) Accuracies were calculated on data from Gao et al. (2002).

Mirão, 2019) and the processes that are responsible for lack of degradation have been subject to scientific research (Friedrich & Degryse, 2019). On the other hand, the burial environment can be a major factor in keeping the good preservation state of the glass fragments (Davison, 2003) or it can be an indication of more recent production date (Posedi, 2020).

The analysis of the major elements of the Ustica glasses (Table 5a) revealed a considerable degree of alteration, although it is not very evident on visual inspection. In fact, most of the fragments have a high silica content ($SiO_2$ > 72% wt) combined with a low alkali content ($Na_2O$ between 3.65–9.7% wt; $K_2O$ between 0.26–2.07% wt). Both chemical characteristics are indicative of de-alkalinization processes detectable in the 12 fragments USPAR-01, 02, 03, 04, 05, 08, 09, 10, 11, 12, 13, and USTRA-04, which we have therefore classified as an *altered group*. The 5 fragments USPAR-06, 07 and USTRA-01, 02, 03 do not show de-alkalization processes, which we have therefore classified as an *unaltered group*. This last group contains two particular cases. The fragment USTRA-03, although characterized by a high content of silica (78.4% wt), has also a high content of sodium (14.43% wt) and therefore it is presumable that it has not undergone the de-alkalinization process. The USPAR-06 fragment has a very high calcium value (25.64% wt) which, as we will see later, make us consider it an authentic *outlier* within the unaltered group.

As most of the fragments analyzed by EPMA-EDS are altered, the LA-ICP-MS data (trace elements) of the pristine glass will be used to understand the original chemical composition and aid to date the fragments. Rubidium and strontium will be used as proxies for potassium and calcium, as an alternative classifying method (Adlington, Freestone, & Teed, 2015; Adlington & Freestone, 2017).

## 5.1 EPMA-EDS

### 5.1.1 Altered Fragments

The EPMA-EDS results of the glass surface indicate the presence of 72.64–85.36 wt% of silica oxide associated with 3.65–9.7 wt% of sodium oxides (Table 5a). These concentrations do not correspond to any known glass composition and can be attributed to the de-alkalization process which is visible in the EPMA images (Figure 6).

**Table 5a:** Major elements in wt% of oxides by EPMA-EDS (**Unaltered**; Altered).

| Sample/Oxide | CaO | Na$_2$O | MgO | Al$_2$O$_3$ | SiO$_2$ | P$_2$O$_5$ | SO$_3$ | ClO | K$_2$O | MnO | FeO |
|---|---|---|---|---|---|---|---|---|---|---|---|
| **USPAR-01** | 6.88 | 3.65 | 0.8 | 3.64 | 80.88 | | 0.18 | 1.51 | 1.25 | 0.56 | 0.65 |
| **USPAR-02** | 6.8 | 5.6 | 1.5 | 3.23 | 78.51 | | 0.15 | 1.76 | 0.88 | 0.82 | 0.75 |
| **USPAR-03** | 9.08 | 8.87 | 2.38 | 1.47 | 76.39 | | 0.1 | 0.38 | 0.8 | 0.23 | 0.29 |
| **USPAR-04** | 5.85 | 3.89 | 1.01 | 2.28 | 85.36 | | 0.24 | - | 0.89 | 0.41 | 0.07 |
| **USPAR-05** | 8.31 | 6.67 | 0.95 | 3.28 | 75.20 | | 0.18 | 1.58 | 1.34 | 1.94 | 0.55 |
| **USPAR-06** | **25.64** | **2.34** | **2.24** | **6.82** | **58.29** | | **-** | **-** | **2.44** | **0.41** | **1.83** |
| **USPAR-07** | **6.62** | **18.82** | **0.75** | **2.28** | **67.69** | | **0.18** | **1.68** | **0.5** | **1.03** | **0.45** |
| **USPAR-08** | 6.13 | 5.01 | 2.21 | 2.09 | 80.09 | | 0.20 | 1.43 | 2.07 | 0.12 | 0.11 |
| **USPAR-09** | 8.82 | 8.76 | 1.05 | 3.57 | 73.93 | | 0.25 | 1.43 | 1.14 | 0.81 | 0.24 |
| **USPAR-10** | 9.09 | 9.04 | 2.49 | 1.75 | 75.62 | | 0.1 | 0.39 | 0.9 | 0.34 | 0.28 |
| **USPAR-11** | 7.35 | 4.48 | 0.66 | 3.51 | 78.82 | | 0.22 | 1.65 | 1.87 | 0.79 | 0.65 |
| **USPAR-12** | 8.33 | 8.18 | 0.41 | 0.98 | 72.76 | | 0.11 | 0.24 | 0.62 | 8.17 | 0.20 |
| **USPAR-13** | 8.18 | 9.7 | 0.34 | 0.42 | 72.64 | | - | 0.13 | 0.26 | 8.08 | 0.25 |
| **USTRA-01** | 7.09 | 6.16 | 4.78 | 10.98 | 64.64 | 0.77 | 0.11 | 0.94 | 3.32 | 0.11 | 1.10 |
| **USTRA-02** | **9.82** | **16.12** | **1.38** | **4.89** | **63.58** | | **0.24** | **0.16** | **1.92** | **0.33** | **1.56** |
| **USTRA-03** | **5.62** | **14.43** | **0.67** | **0.04** | **78.40** | | **-** | **0.54** | **0.3** | **-** | **-** |
| **USTRA-04** | **8.89** | **7.71** | **0.71** | **3.44** | **75.43** | | **0.2** | **0.31** | **2.84** | **0.26** | **0.21** |
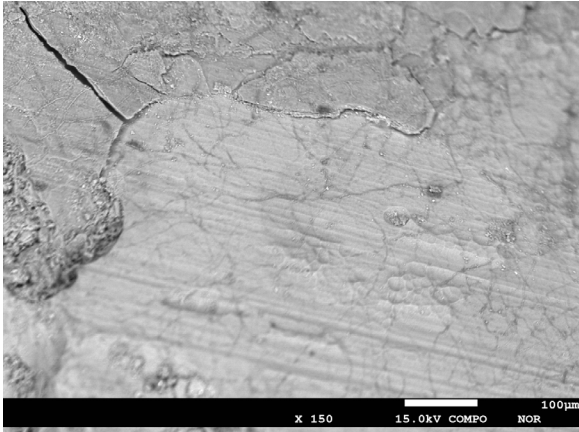
**Figure 6:** EPMA image of a de-alkalized surface of fragment USPAR-08.

The Ustica fragments composition can be correlated to the measurement of a deteriorated surface of soda glass described in the literature (Orlando, Olmi, Vaggelli, & Bacci, 1996; Silvestri, Molin, & Salviulo, 2005; Barbera, Barone, Crupi, Longo, Majolino, Mazzoleni, Sabatino, Tanasi, & Venuti, 2012). In particular, the altered glass of Ustica shows some affinities with those of the Pisa Cathedral described by Orlando et al. (1996). In both Ustica and Pisa Cathedral samples, it is evident that there is a high depletion of alkali (soda and potassium oxides) which is associated with low depletion of calcium and enrichment in silica. In the case of the Pisa Cathedral samples the pristine cross-section has been analyzed in addition to surface analysis and those results confirm that the pristine glass chemical data is well within the range of values known for soda glass (Orlando et al., 1996).

In our case, magnesium and potassium values of 12 altered fragments have been used as a provisional marker of the flux used (Figure 7). In the case where either or both magnesium and potassium values are above 1.5 wt%, the attributed flux is plant-ash (soda or mixed-alkali glass). On the contrary, if both magnesium and potassium values are below 1.5 wt% the flux cannot be attributed to natron, soda plant-ash nor mixed-alkali plant ash as we do not understand the severity of depletion of these elements at this point.
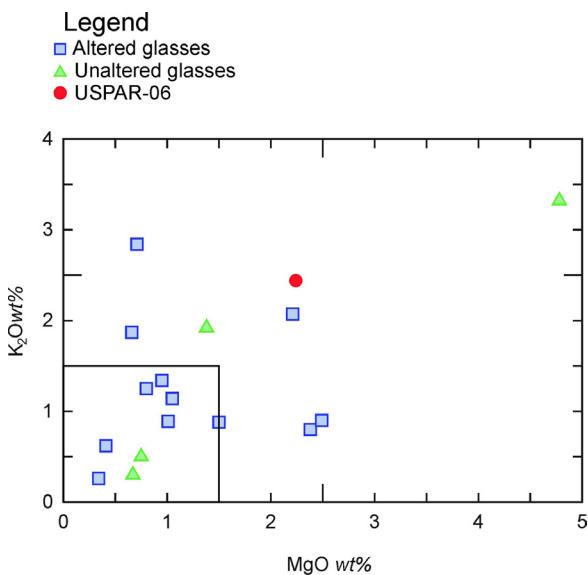


**Figure 7:** MgO vs $K_2O$ binary plot highlights the fragments of glass whose values are above 1.5 wt% and that were produced with a plant ash flux.

**Table 5b:** Trace element concentrations in ppm determined by LA-ICP-MS. Each concentration is the average value of three measurements; * the average value of two measurements. StDev=standard deviation.

| | Ti | V | Cr | Co | Cu | Ni | Zn | As | Rb | Sr | Y | Zr | Nb | Sn | Sb | Ba | Pb |
|---|---|---|---|---|---|---|---|---|---|---|---|---|---|---|---|---|---|
| USPAR-01 | 509 | 19.1 | 21.0 | 20.8 | 830 | 8.97 | 37.22 | 17.1 | 9.40 | 415 | 6.11 | 41.3 | 1.72 | 85 | 2610 | 257 | 934 |
| *StDev* | 27 | 1.25 | 3.36 | 1.97 | 53 | 0.50 | 5.66 | 2.68 | 0.70 | 22.1 | 0.41 | 1.94 | 0.25 | 9.36 | 240 | 12.6 | 84 |
| USPAR-02 | 838 | 21.6 | 15.6 | 5.76 | 33 | 7.01 | 33.52 | 6.00 | 3.99 | 527 | 6.99 | 67.1 | 2.53 | 1.35 | 1.16 | 399 | 17.3 |
| *StDev* | 32 | 1.13 | 1.65 | 0.48 | 4.4 | 0.91 | 4.19 | 0.40 | 0.11 | 9.91 | 0.39 | 1.61 | 0.10 | 0.19 | 0.12 | 14.9 | 1.88 |
| USPAR-03 | 455 | 7.88 | 49.9 | 284 | 386 | 16.0 | 57.71 | 459 | 15.0 | 106 | 3.79 | 102 | 1.93 | 22.5 | 785 | 209 | 1603 |
| *StDev* | 18 | 0.72 | 6.59 | 17.4 | 33 | 1.91 | 5.38 | 20.5 | 1.19 | 4.25 | 0.31 | 4.75 | 0.21 | 2.28 | 51 | 19.9 | 163 |
| USPAR-04 | 177 | 2.86 | 10 | 967 | 18 | 15.0 | 265 | 1286 | 1.93 | 44.5 | 1.11 | 25.2 | 0.79 | 1.89 | 1644 | 4029 | 155 |
| *StDev* | 9 | 0.25 | | 53.5 | 2.2 | 1.67 | 17.22 | 84 | 0.18 | 4.07 | 0.09 | 1.60 | 0.01 | 0.17 | 81 | 209 | 2.26 |
| USPAR-05 | 438 | 19.4 | 18.1 | 608 | 285 | 15.7 | 31.31 | 5.23 | 8.72 | 538 | 6.89 | 35.3 | 1.22 | 267 | 7.86 | 240 | 807 |
| *StDev* | 37 | 1.02 | 1.33 | 14.3 | 22 | 1.82 | 4.08 | 0.38 | 0.37 | 10.06 | 0.40 | 1.41 | 0.17 | 10.17 | 0.64 | 5.94 | 4.43 |
| USPAR-07 | 549 | 15.7 | 15.0 | 9.41 | 155 | 6.48 | 16.89 | 5.70 | 5.80 | 384 | 5.51 | 39.7 | 1.39 | 12.14 | 233 | 314 | 261 |
| *StDev* | 40 | 0.50 | 1.80 | 0.66 | 15 | 0.80 | 1.85 | 0.65 | 0.24 | 17.1 | 0.22 | 2.63 | 0.13 | 0.43 | 7.78 | 12.1 | 11.18 |
| USPAR-08 | 111 | 6.80 | 7.47 | 3.81 | 15 | 3.02 | 13.62 | 202 | 6.14 | 39.1 | 0.80 | 7.42 | 0.56 | 14.11 | 46.3 | 176 | 1033 |
| *StDev* | 14 | 0.57 | 0.41 | 0.43 | 1.9 | 0.19 | 1.91 | 8.87 | 0.39 | 2.12 | 0.07 | 0.57 | 0.07 | 1.37 | 2.27 | 3.69 | 72 |
| USPAR-09 | 275 | 12.8 | | 7.02 | 32 | 7.25 | 12.65 | 3.79 | 7.89 | 492 | 6.72 | 23.7 | 1.06 | 1.76 | 7.46 | 199 | 11.28 |
| *StDev* | 19 | 1.06 | | 0.92 | 4.4 | 1.00 | 1.93 | 0.41 | 0.37 | 18.32 | 0.74 | 2.15 | 0.11 | 0.15 | 0.97 | 4.02 | 0.57 |
| USPAR-10 | 347 | 10 | 66 | 265 | 379 | 16.8 | 49.16 | 492 | 34.9 | 102 | 3.38 | 95 | 2.05 | 18.07 | 692 | 158 | 1518 |
| *StDev* | 42 | 1.21 | 8.3 | 32.8 | 42 | 2.18 | 5.49 | 41.8 | 4.09 | 8.19 | 0.46 | 9.30 | 0.29 | 1.12 | 96 | 18.4 | 115 |
| USPAR-11 | 625 | 26 | 29.7 | 69 | 1367 | 17.9 | 32.78 | 4979 | 11.85 | 457 | 7.36 | 47 | 1.69 | 116 | 3731 | 300 | 1805 |
| *StDev* | 86 | 3.34 | 3.9 | 6.68 | 127 | 2.19 | 3.80 | 131 | 1.60 | 23.2 | 0.73 | 4.66 | 0.14 | 16.12 | 468 | 35.3 | 166 |
| USPAR-12 | 223 | 36.9 | | 583 | 100 | 65 | 267 | 4981 | 1.90 | 87 | 4.54 | 31.8 | 0.62 | 1.91 | 23.6 | 847 | 220 |
| *StDev* | 18 | 2.37 | | 43 | 2.3 | 9.02 | 11.19 | 249 | 0.29 | 8.43 | 0.46 | 1.98 | 0.08 | 0.10 | 2.69 | 49 | 7.74 |
| USPAR-13* | 244 | 38.5 | | 565 | 107 | 67 | 266 | 4979 | 1.42 | 85 | 3.91 | 30.9 | 0.76 | 10.5 | 96 | 790 | 238 |
| *StDev* | 19 | 1.78 | | 4.31 | 6.7 | 0.90 | 14.15 | 131 | 0.13 | 0.74 | 0.47 | 2.63 | 0.05 | 1.41 | 1.33 | 22.4 | 36 |
| USTRA-01 | 644 | 26.8 | 29.1 | 3.94 | 31 | 9.99 | 43.4 | 14.4 | 35 | 137 | 6.31 | 42 | 4.35 | 7.80 | 2.07 | 140 | 97 |
| *StDev* | 5 | 3.52 | 3.0 | 0.51 | 4.0 | 0.87 | 5.31 | 1.80 | 3.24 | 7.33 | 0.78 | 1.84 | 0.41 | 1.11 | 0.28 | 15.8 | 8.14 |
| USTRA-02 | 437 | 29.3 | | 6.52 | 22 | 34 | 36.2 | 25.3 | 73 | 348 | 6.88 | 54.5 | 2.60 | 8.17 | 1.99 | 469 | 29.5 |
| *StDev* | 47 | 3.44 | | 0.74 | 3.9 | 4.20 | 4.64 | 3.24 | 8.14 | 41.6 | 0.72 | 6.32 | 0.33 | 0.56 | 0.25 | 54 | 4.20 |
| USTRA-03 | 97 | 4.07 | | 2.19 | 4.2 | 9.30 | 34.5 | 3991 | 0.73 | 22.5 | 0.89 | 27.9 | 0.70 | - | 1042 | 25.8 | 36.8 |
| *StDev* | 5 | 0.44 | | 0.29 | 0.5 | 1.18 | 4.45 | 358 | 0.06 | 1.80 | 0.01 | 1.61 | 0.06 | - | 74 | 3.32 | 4.57 |
| USTRA-04 | 347 | 6.68 | 15.2 | 452 | 102 | 24.1 | 52.2 | 315 | 39.64 | 83 | 2.92 | 49.7 | 2.13 | 23.0 | 50.7 | 192 | 481 |
| *StDev* | 42 | 0.74 | 1.7 | 25.0 | 6 | 2.22 | 7.16 | 31.0 | 1.60 | 1.17 | 0.36 | 1.93 | 0.23 | 3.06 | 6.41 | 4.93 | 37.4 |

**Table 5b. Continued.**

| | La | Ce | Pr | Nd | Sm | Eu | Gd | Tb | Dy | Ho | Er | Tm | Yb | Lu |
|---|---|---|---|---|---|---|---|---|---|---|---|---|---|---|
| USPAR-01 | 5.99 | 10.37 | 1.38 | 5.30 | 0.72 | 0.38 | 1.24 | 0.19 | 1.08 | 0.20 | 0.71 | 0.09 | 0.71 | 0.11 |
| *StDev* | *0.56* | *0.33* | *0.15* | *0.45* | *0.07* | *0.04* | *0.13* | *0.02* | *0.06* | *0.02* | *0.09* | *0.01* | *0.07* | *0.01* |
| USPAR-02 | 7.16 | 11.80 | 1.55 | 6.16 | 1.02 | 0.40 | 1.53 | 0.12 | 0.88 | 0.23 | 0.80 | 0.15 | 0.94 | 0.16 |
| *StDev* | *0.53* | *1.09* | *0.19* | *0.76* | *0.13* | *0.02* | *0.16* | *0.01* | *0.03* | *0.02* | *0.07* | *0.02* | . | *0.02* |
| USPAR-03 | 5.72 | 10.34 | 1.06 | 4.39 | 0.99 | 0.33 | 0.82 | 0.13 | 0.87 | 0.18 | 0.74 | 0.09 | . | . |
| *StDev* | *0.61* | *0.93* | *0.09* | *0.57* | *0.08* | *0.25* | . | *0.00* | *0.07* | *0.01* | *0.03* | . | . | . |
| USPAR-04 | 1.00 | 1.83 | 0.19 | 0.89 | 0.72 | 0.14 | 0.61 | 0.11 | 0.35 | 0.07 | 0.24 | . | . | 0.10 |
| *StDev* | *0.14* | *0.12* | *0.01* | *0.13* | *0.06* | *0.01* | . | *0.02* | *0.04* | *0.00* | . | . | . | *0.00* |
| USPAR-05 | 6.14 | 10.31 | 1.59 | 6.43 | 1.11 | 0.38 | 1.01 | 0.14 | 1.45 | 0.18 | 0.69 | 0.08 | 1.01 | 0.16 |
| *StDev* | *0.60* | *0.34* | *0.13* | *0.76* | *0.12* | *0.03* | *0.15* | *0.02* | *0.11* | *0.02* | *0.11* | . | *0.11* | *0.02* |
| USPAR-07 | 5.23 | 9.17 | 1.06 | 5.29 | 1.06 | 0.35 | 1.13 | 0.14 | 0.82 | 0.22 | 0.39 | 0.12 | 0.83 | 0.08 |
| *StDev* | *0.12* | *0.58* | *0.09* | *0.67* | *0.04* | *0.05* | *0.08* | *0.01* | *0.09* | *0.03* | *0.03* | *0.01* | *0.08* | *0.01* |
| USPAR-08 | 0.90 | 1.95 | 0.20 | 0.88 | 0.21 | 0.10 | 0.49 | . | 0.17 | 0.05 | . | 0.03 | . | 0.05 |
| *StDev* | *0.11* | *0.24* | *0.02* | *0.09* | *0.01* | *0.01* | *0.01* | . | *0.01* | *0.01* | . | *0.00* | . | *0.01* |
| USPAR-09 | 4.85 | 9.79 | 1.21 | 6.12 | 1.18 | 0.23 | 1.03 | . | 1.04 | 0.40 | 0.68 | 0.12 | 0.93 | 0.10 |
| *StDev* | *0.59* | *0.42* | *0.13* | *1.18* | *0.11* | *0.03* | *0.08* | . | *0.10* | *0.06* | *0.06* | *0.01* | *0.09* | *0.01* |
| USPAR-10 | 5.62 | 14.15 | 0.91 | 4.72 | 2.89 | 0.55 | . | . | 1.18 | 0.26 | 0.66 | 0.07 | . | 0.33 |
| *StDev* | *0.67* | *1.92* | *0.04* | *0.48* | *0.30* | *0.02* | . | . | *0.10* | *0.03* | *0.01* | *0.01* | . | *0.04* |
| USPAR-11 | 6.03 | 12.02 | 2.11 | 6.15 | 1.51 | 0.56 | 2.38 | 0.23 | 1.32 | . | 2.39 | 0.38 | 2.41 | 0.32 |
| *StDev* | *0.68* | *1.12* | *0.19* | *0.83* | *0.17* | *0.07* | *0.17* | *0.03* | *0.10* | . | *0.18* | *0.05* | *0.23* | *0.05* |
| USPAR-12 | 5.73 | 6.90 | 2.33 | 8.97 | 0.66 | . | 1.14 | 0.15 | 0.87 | 0.16 | 1.03 | 0.14 | 1.14 | 0.07 |
| *StDev* | *0.75* | *0.47* | *0.13* | *0.66* | *0.01* | . | *0.06* | *0.02* | *0.01* | *0.01* | *0.09* | *0.01* | *0.01* | *0.01* |
| USPAR-13* | 5.46 | 10.06 | 2.57 | 7.59 | 2.53 | 0.31 | 1.29 | 0.42 | 1.54 | 0.91 | . | . | . | . |
| *StDev* | *0.63* | *5.15* | *0.10* | *0.92* | *0.01* | *0.01* | *0.01* | *0.29* | *0.10* | *0.10* | . | . | . | . |
| USTRA-01 | 7.56 | 18.43 | 2.08 | 7.25 | 1.65 | 0.43 | 1.01 | 0.19 | 0.95 | 0.30 | 0.67 | 0.15 | 0.47 | 0.27 |
| *StDev* | *0.93* | *1.50* | *0.25* | *0.94* | *0.18* | *0.02* | *0.07* | *0.02* | *0.13* | *0.03* | *0.10* | *0.02* | *0.01* | *0.03* |
| USTRA-02 | 11.78 | 22.06 | 3.71 | 15.63 | 6.18 | 2.23 | 4.51 | 1.31 | 3.10 | . | 4.09 | 2.28 | 8.05 | . |
| *StDev* | *1.44* | *2.69* | *1.18* | *12.91* | *0.50* | *0.30* | *.51* | *0.18* | *0.23* | . | *0.50* | *0.26* | *0.96* | . |
| USTRA-03 | 0.61 | 1.18 | 0.46 | . | . | 0.45 | . | 0.11 | 1.57 | 0.30 | 0.41 | 0.13 | . | 0.25 |
| *StDev* | *0.05* | *0.07* | *0.05* | . | . | *0.05* | . | *0.01* | *0.20* | *0.03* | *0.03* | *0.02* | . | *0.03* |
| USTRA-04 | 3.48 | 6.37 | 0.80 | 3.04 | 1.40 | . | 1.33 | 0.28 | 1.07 | 0.14 | 0.84 | . | 0.87 | 0.27 |
| *StDev* | *0.23* | *0.41* | *0.07* | *0.46* | *0.13* | . | *0.14* | *0.03* | *0.02* | *0.02* | *0.06* | . | *0.05* | *0.03* |

**Table 5c:** Trace element concentrations in ppm determined by LA-ICP-MS normalized to Continental Crust (Continental Crust data taken from Wedepohl, 1995). Each concentration is the average value of three measurements; * the average value of two measurements.

| | La | Ce | Pr | Nd | Sm | Eu | Gd | Tb | Dy | Ho | Er | Tm | Yb | Lu |
|---|---|---|---|---|---|---|---|---|---|---|---|---|---|---|
| USPAR-01 | 0.20 | 0.17 | 0.21 | 0.20 | 0.14 | 0.29 | 0.31 | 0.29 | 0.29 | 0.25 | 0.34 | 0.29 | 0.35 | 0.30 |
| USPAR-02 | 0.24 | 0.20 | 0.23 | 0.23 | 0.19 | 0.31 | 0.38 | 0.19 | 0.23 | 0.29 | 0.38 | 0.51 | 0.47 | 0.46 |
| USPAR-03 | 0.19 | 0.17 | 0.16 | 0.16 | 0.19 | 0.26 | 0.21 | 0.21 | 0.23 | 0.23 | 0.35 | 0.30 | 0.00 | 0.00 |
| USPAR-04 | 0.03 | 0.03 | 0.03 | 0.03 | 0.13 | 0.11 | 0.15 | 0.17 | 0.09 | 0.08 | 0.11 | 0.00 | 0.00 | 0.27 |
| USPAR-05 | 0.20 | 0.17 | 0.24 | 0.24 | 0.21 | 0.29 | 0.25 | 0.22 | 0.38 | 0.22 | 0.33 | 0.26 | 0.50 | 0.46 |
| USPAR-07 | 0.17 | 0.15 | 0.16 | 0.20 | 0.20 | 0.27 | 0.28 | 0.22 | 0.21 | 0.28 | 0.19 | 0.41 | 0.41 | 0.24 |
| USPAR-08 | 0.03 | 0.03 | 0.03 | 0.03 | 0.04 | 0.08 | 0.12 | 0.00 | 0.04 | 0.07 | 0.00 | 0.11 | 0.00 | 0.14 |
| USPAR-09 | 0.16 | 0.16 | 0.18 | 0.23 | 0.22 | 0.18 | 0.26 | 0.00 | 0.27 | 0.50 | 0.32 | 0.39 | 0.47 | 0.27 |
| USPAR-10 | 0.19 | 0.24 | 0.14 | 0.17 | 0.55 | 0.42 | 0.00 | 0.00 | 0.31 | 0.33 | 0.31 | 0.24 | 0.00 | 0.94 |
| USPAR-11 | 0.20 | 0.20 | 0.31 | 0.23 | 0.29 | 0.43 | 0.60 | 0.36 | 0.35 | 0.00 | 1.14 | 1.27 | 1.20 | 0.93 |
| USPAR-12 | 0.19 | 0.12 | 0.35 | 0.33 | 0.12 | 0.00 | 0.28 | 0.23 | 0.23 | 0.20 | 0.49 | 0.47 | 0.57 | 0.20 |
| USPAR-13* | 0.18 | 0.17 | 0.38 | 0.28 | 0.48 | 0.24 | 0.32 | 0.64 | 0.41 | 1.14 | 0.00 | 0.00 | 0.00 | 0.00 |
| USTRA-01 | 0.25 | 0.31 | 0.31 | 0.27 | 0.31 | 0.33 | 0.25 | 0.28 | 0.25 | 0.37 | 0.32 | 0.49 | 0.24 | 0.77 |
| USTRA-02 | 0.39 | 0.37 | 0.55 | 0.58 | 1.17 | 1.72 | 1.13 | 2.01 | 0.82 | 0.00 | 1.95 | 7.60 | 4.03 | 0.00 |
| USTRA-03 | 0.02 | 0.02 | 0.07 | 0.00 | 0.00 | 0.35 | 0.00 | 0.17 | 0.41 | 0.38 | 0.19 | 0.45 | 0.00 | 0.71 |
| USTRA-04 | 0.12 | 0.11 | 0.12 | 0.11 | 0.26 | 0.00 | 0.33 | 0.44 | 0.28 | 0.17 | 0.40 | 0.00 | 0.44 | 0.76 |

### 5.1.2 Unaltered Fragments

Fragments USPAR-07 and USTRA-02 have both silica oxide and sodium oxide values that are characteristic of silica-soda-lime glasses widely used from the Roman period until the Medieval period (Table 5a). USPAR-07 shows low magnesium oxide and potassium oxide values (<1.5 wt%) indicating natron being used as a flux (Figure 7). On the other hand, USTRA-02 has lower magnesium (1.38 wt%) and higher potassium content (1.92 wt%) (Figure 7). This could indicate the use of plant-ash or mixing it with natron, possibly through recycling for which we would need a larger assemblage of samples of this type to confirm through correlations of potassium, magnesium and phosphorus oxide with natron (Freestone et al., 2008).

Fragment USTRA-01 has extremely high aluminum values of 10.98 wt% combined with low sodium oxide (6.16 wt%), high calcium oxide (7.09 wt%) and low strontium (137 ppm) (Table 5a,b). Along with earth-alkali oxides, aluminum oxide is known to be a good stabilizer of glass (Brill, 1962; Pollard & Heron, 2008; Shackelford & Doremus, 2008; Rapp, 2009; Wedepohl, Simon, & Kronz, 2011; Janssens, 2013). This extremely high amount of alumina combined with high calcium would make a durable glass that is not prone to heavy degradation (Farges, Etcheverry, Scheidegger, & Grolimund, 2006; Palomar, 2018). High alumina soda glasses are generally not found frequently, but they are recognized in assemblages such as 2nd/1st century BC–5th century AD glass beads from Sri Lanka and South India (Dussubieux, Gratuze, & Blet-Lemarquand, 2010, tab. 4; Dussubieux & Gratuze, 2013; Carter, 2016) which were present in Early Roman Quseir, Egypt (Then-Obłuska & Dussubieux, 2016) and during Early Byzantine period in Europe (Poulain, Sciuller, & Gratuze, 2013; Pion & Gratuze 2016); 4th–6th century AD glass beads from upper Nubia in Africa (Then-Obłuska, Wagner, & Kepa-Linowska, 2019); 7th–8th century AD Asian glass beads imported to Scandinavia and north Germany (Sode, Gratuze, & Lankton, 2017); 7th–10th century AD in Zanzibar (Wood, Panighello, Orsega, Robertshaw, van Elteren Crowther, Horton, & Boivin, 2017); 8th–12th century AD glass

bracelets from Ḥiṣn al-Tīnātand in Turkey (Swan, Rehren, Dussubieux, & Eger, 2018). Few red opaque glass beads of Asian production found in Scandinavia and northern Germany (defined as group 4) show the most similarity with USTRA-01 as both calcium and aluminum values are around 10 wt% (Sode et al., 2017, Figure 5). These red glass beads are colored with 1–5 wt% of copper oxide and have the presence of tin and some antimony which is not the case of USTRA-01. Considering all the archaeological and compositional data, USTRA-01 could be associated with the Byzantine settlement.

USPAR-06 is the only HLLA (High Lime Low Alkali) glass with high calcium oxide (25.64 wt%) and aluminum oxide (6.82 wt%) and very low potassium oxide (2.44 wt%), sodium oxide (2.34 wt%) and magnesium oxide (2.24 wt%) (Table 5a). Parallels to similar major and minor chemical composition can be found in glass bottles from the 17th–18th century AD Lisbon (Coutinho, Gratuze, Alves, Medici, & Vilarigues, 2017).

Finally, the USTRA-03 fragment shows a high silica oxide (78.4 wt%) and sodium oxide (14.43 wt%) contents (Table 5a). It does not display any sign of deterioration, although calcium oxide levels are in the lower range (5.62 wt%) for a soda-based glass. The extremely low levels of aluminum oxide (0.04 wt%), and chlorine, iron and manganese oxides below the detection limit of the instrument are a strong indication of USTRA-03 being a modern synthetic soda glass which needs to be further confirmed by LA-ICP-MS.

## 5.2 LA-ICP-MS

### 5.2.1 Raw Materials Origin

For a better understanding of which raw materials were used and to understand the nature and provenance of the glass fragments, trace elements including Rare Earth Elements (REE's) were examined.

As noted before, rubidium and strontium were used as proxies for potassium and calcium to determine the raw material source (Adlington et al., 2015; Adlington & Freestone, 2017). The binary diagram of rubidium and strontium shows three clusters and two outliers (Figure 8).
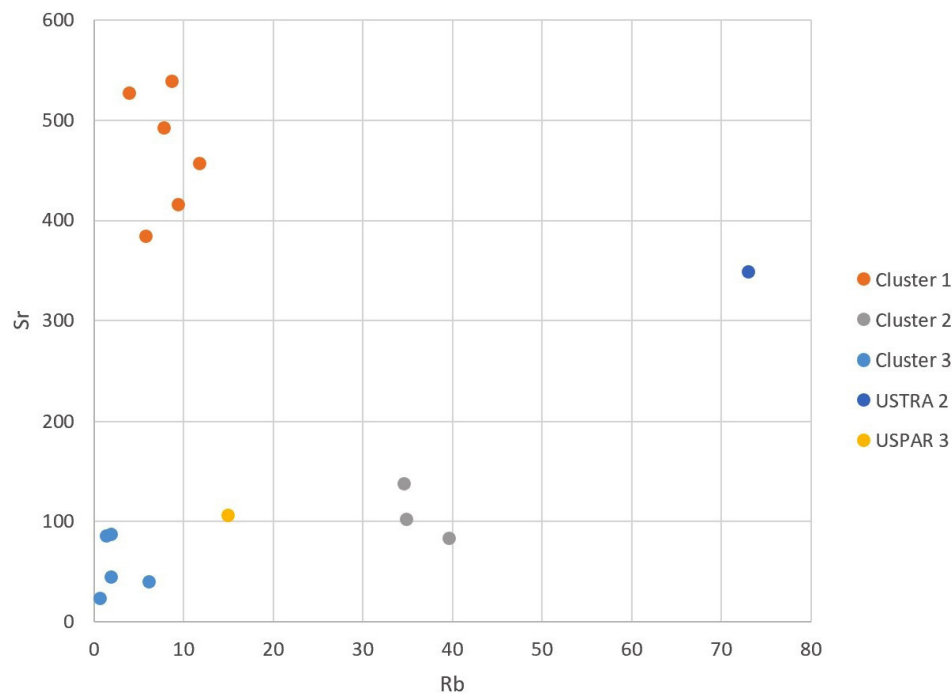


**Figure 8:** Three clusters and two outliers are defined, based on rubidium and strontium which were used as proxies respectively for potassium and calcium.

Cluster 1 includes fragments USPAR-01, 02, 05, 07, 09 and 11, characterized by very low rubidium (4–12 ppm) and high strontium (384–538 ppm). This is indicative of the soda-lime glass characteristic of the Roman and Early Medieval periods (Barca et al., 2016; Freestone, Degryse, Lankton, Gratuze, & Schneider, 2018; Hellemans, Cagno, Bogana, Janssens, & Mendera, 2019).

Cluster 2 includes fragments USPAR-10, USTRA-01 and 04. They have higher rubidium (35–40 ppm) and lower strontium (83–137 ppm) which should be a result of the use of plant-ashes. These levels are present in the 14th century AD San Vettore fragment (Cagno, Mendera, Jeffries, & Janssens, 2010) and 17th century AD colorless vessels from Florence (Brill 1999a, Brill 1999b). The 7th–8th century AD red opaque high alumina-high lime Asian beads (group 4) found in Scandinavia have a strontium level (circa 80 ppm; Sode et al., 2017, Figure 6) which are within the range of the USTRA-01 and Cluster 2 in general. Unfortunately, there is no information about their rubidium contents which does not make a comparison with USTRA-01 complete and it does not validate the age nor provenance of USTRA-01.

Cluster 3 includes fragments USPAR-04, 08, 12, 13 and USTRA-03 that have very low rubidium (<6 ppm) and strontium (<50 ppm) reflecting the lack of potassium and presence of a small amount of calcium. Both very low potassium and calcium are not characteristic of Roman and Medieval glasses. A parallel to low amounts of rubidium and strontium are found in English synthetic soda glass dated to the 19th and 20th centuries AD (Dungworth, 2017). Therefore, we can attribute this group to post-medieval/modern synthetic soda samples.

Interestingly, clusters 2 and 3 show a strong positive correlation of yttrium and strontium ($R^2$=0.92; $R^2$=0.95), while there is no strong positive correlation within cluster 1 ($R^2$=0.56) (Figure 9). A strong positive correlation between yttrium and strontium must be associated with the calcium source. In calcium-based minerals, Ca atoms can be replaced by strontium and yttrium in trace quantities, due to the comparability of their ionic radii (ca. 1 Angstrom). But while strontium is vicariant of Ca both in calcium carbonates (i.e. calcite, dolomite) and in calcium phosphates (i.e. apatite), Yttrium preferentially replaces calcium in phosphates (Gueriau, Jauvion, & Mocuta, 2018, and references therein). Therefore, the strong correlation between Sr and Y in clusters 2 and 3 could indicate the presence in the glass not only of calcium carbonates but also of phosphates. Carbonates and phosphates of biogenic origin are present in the shells and skeletons of marine organisms (Gueriau et al. 2018, and references therein) and they may have arrived in the glass recipe through the siliceous sand.

A strong positive correlation is noted between titanium and niobium in clusters 1 ($R^2$=0.87) and 2 ($R^2$=0.99) (Figure 10). A moderate positive correlation between iron and titanium in clusters 1 and 3 ($R^2$=0.74; $R^2$=0.73), and a strong positive correlation in cluster 2 ($R^2$=0.99). Cluster 1 also displays a strong positive correlation between titanium and zirconium ($R^2$=0.97) (Figure 11).

All these elements are considered to be impurities in the silica source and a positive correlation of iron and titanium, titanium and niobium, titanium and zirconium indicate the presence of columbite ($FeNb_2O_6$) which is selectively deposited with Fe–Ti bearing oxide minerals (zircon and ilmenite) (Posedi et al. 2019 and references therein). Columbite minerals are common in the areas where granitic rock outcrops can be found (Scott Ercit, 1994; Abdalla, Helba, Mohamed, 1998; Posedi et al. 2019 and references therein).

REEs (La-Lu; normalized values used) of each sample in each cluster do not overlap with each other indicating different provenance of the raw material or that the recycling and addition of cullet have changed the REE pattern drastically. Fragments USPAR-04, 12 and 13 from cluster 3, USTRA-04 from cluster 2 and USPAR-09 from cluster 1 have a negative Eu anomaly which usually interpreted as evidence of earlier separation of a mineral phase such as Ca-plagioclases (Posedi et al., 2019 and references therein).

Comparing trace elements pattern of rubidium, strontium, yttrium, zirconium, barium, lanthanum, cerium, praseodymium, neodymium and thorium between each of the clusters, cluster 1 is compatible to Levantine I and Jarrow glasses (Freestone, 2005) (Figure 12).
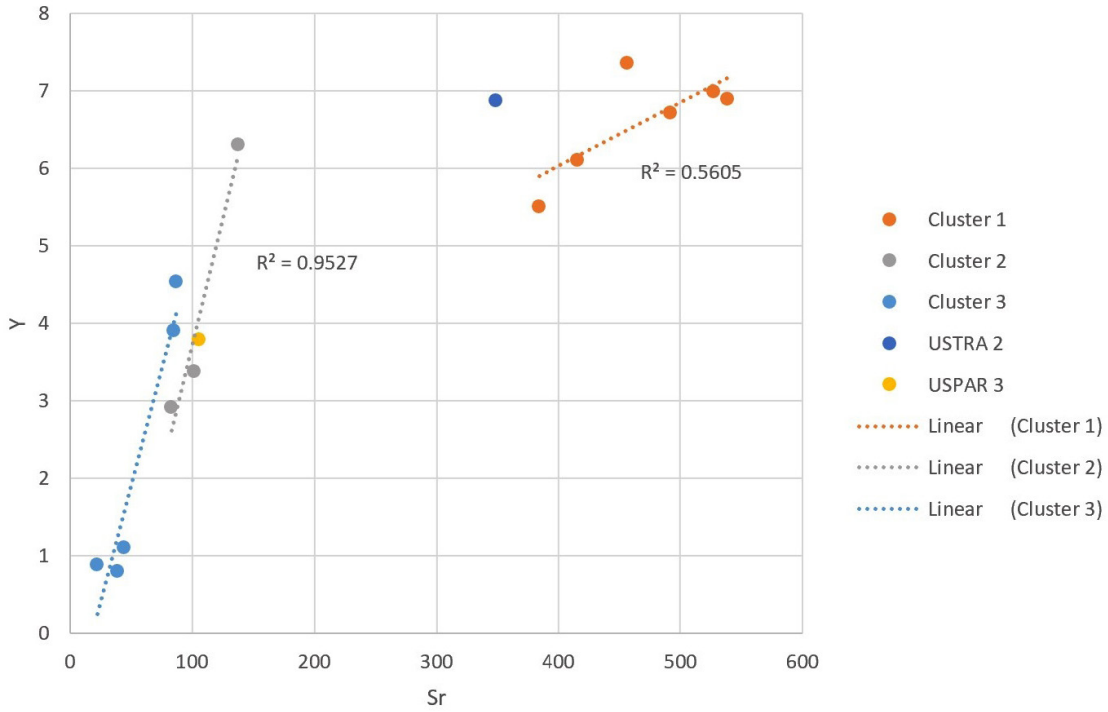
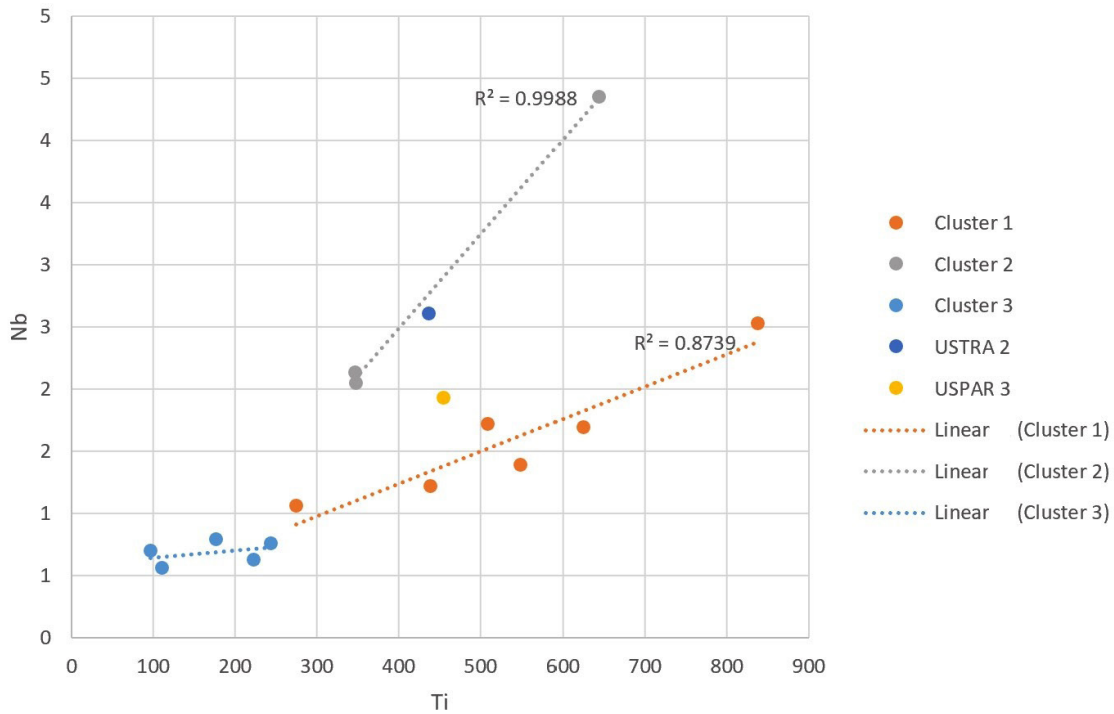**Figure 9:** Correlation of strontium and yttrium according to clusters.



**Figure 10:** Correlations of titanium and niobium in three clusters.
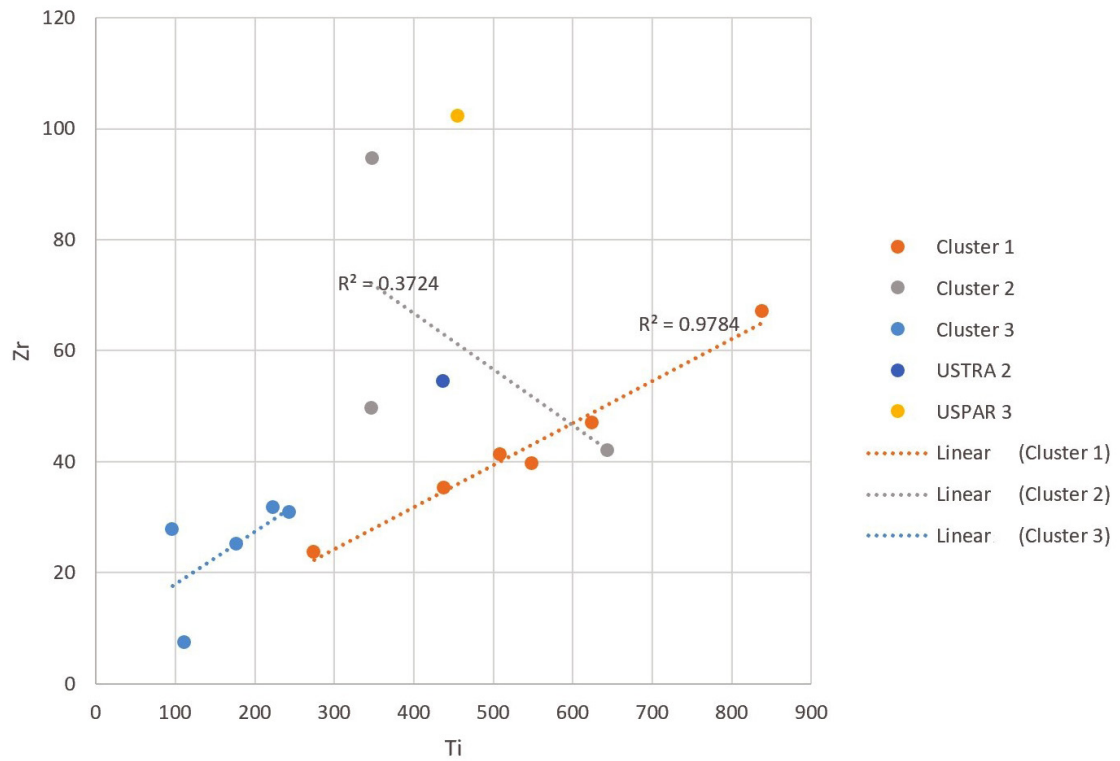
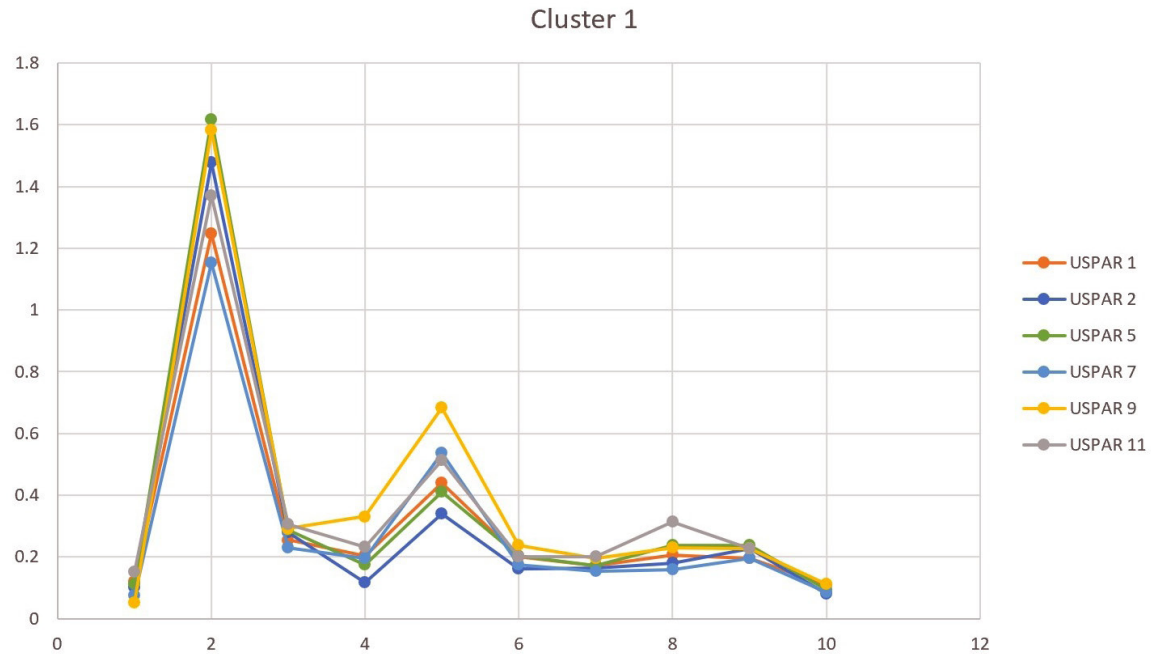**Figure 11:** Correlations of titanium and zirconium in three clusters.



**Figure 12:** The signature characteristic of cluster 1. The same pattern is noted in Roman Levantine I and Early Medieval Jarrow glass fragments as presented in Freestone (2005).

### 5.2.2 (De)colorants and Recycling

The assemblage contains fragments of colorless/tinted green and yellow, purple, blue and green-blue (Table 3).

#### 5.2.2.1 Cluster 1

Tinted green and blue-green fragments USPAR-01, USPAR-07, USPAR-11 have elevated amounts of copper (155–1367 ppm), antimony (233–3731 ppm) and lead (261–1805 ppm), and in the case of USPAR-11 tin (116 ppm) as well. Due to the small amount of these elements comparing to the amount found in Roman tesserae (Barca et al., 2016; 2019), the weakly colored appearance of the fragments and a positive correlation of antimony and copper prove that a green colored tesserae was added to the batch confirming the practice of recycling. The elevation of these elements in the weakly colored glass is encountered on various sites such as San Vincenzo al Volturno (Schibille & Freestone, 2013) and Crypta Balbi in Rome (Mirti, Lepora, & Sagui, 2000). USPAR-05 is a deep blue colored fragment colored with cobalt (608 ppm). USPAR-02 and USPAR-09 are colorless, indeed they have no elevated concentrations of trace elements that indicate the absence of recycling or intentional addition of colorants.

#### 5.2.2.2 Cluster 2

Blue fragments USTRA-04 and USPAR-10 has elevated cobalt (265–452 ppm) associated with elevated copper (102–379 ppm), arsenic (315–492 ppm), antimony (51–692 ppm) and lead (481–1518 ppm). The amount of the aforementioned trace elements indicates the addition of blue tesserae as cullet. The elevated arsenic associated with elevated lead, copper and antimony (and cobalt when discussing blue glass) is present in Siena Cathedral stained-glass window made by Duccio di Buoninsegna dated to late 13th century AD (1288–1289 AD) (Basso, Riccardi, Messiga, Mendera, Gimeno, Garcia-Valles, Fernandez-Turiel, Bazzocchi, Aulinas, & Tarozzi, 2009). USTRA-01 appears to be made from scratch without any addition of glass cullet to the batch. No colorants have been added and the deep green color seems to be obtained due to presence of iron (1.10 wt%) and a very small amount of manganese (0.11 wt%) in combination with furnace conditions.

#### 5.2.2.3 Cluster 3

Purple in fragments USPAR-12 and USPAR-13 is obtained by high amounts of manganese (respectively 8.17 wt% and 8.08 wt%). Alongside manganese, there is enough cobalt (565–583 ppm) to achieve the deep blue color and it is associated with high arsenic (av 4980 ppm). The association of cobalt and arsenic only appears from the 16th–18th centuries and it is provenanced to Schneeberg (Saxony, Germany) (Gratuze, Soulier, Barrandon, & Foy, 1992, 1995). This locality is confirmed by the contemporary written sources and it is a place where, in 1520 AD, Peter Weidenhammer discovered smalt (Gratuze et al., 1992, 1995). The pinkish color in glass fragment USTRA-03 is achieved due to the amount of manganese (1399 ppm) exceeding the amount of iron (268 ppm). In particular, the manganese and iron contents for this sample are below the detection limit of EPMA-EDS (Table 5a), therefore their concentrations have been determined by LA-ICP-MS. In addition, USTRA-03 shows an elevated amount of arsenic (3991 ppm) and antimony (1042 ppm) which could have been added as decolorants. The correlation of these elevated amounts of arsenic and antimony can also be found in synthetic soda stained glass from Beverly Minster in England (Dungworth, Bower, Gilchrist, & Wilkes, 2010). When arsenic ($As_2O_3$) present in the glass with less than 0.5 wt% it has the role to decolorize and refine glass (Verità & Zecchin, 2016). It was used in the glass batches in Murano from the end of the 17th and the beginning of the 18th century AD (Verità & Zecchin, 2016) until 2015 (Trouth, 2017). Finally, the fragment has very low amounts of copper, cobalt, nickel, zinc, tin, and lead (all <100 ppm) indicating a lack of recycling. Fragment USPAR-08 is tinted green it has an amount of iron oxide (0.11 wt%) similar to the amount of manganese oxide (0.12wt%), no antimony (42 ppm), a small amount of arsenic (202 ppm) and elevated lead (1033 ppm). Possibly lead arsenate was added as a refining agent or colorant but the decolorization was not successful.

Very low titanium (<200 ppm) in fragments USPAR-04, USPAR-08 and USTRA-03 seem to be discriminated from the rest of the set as these low values are characteristic of modern glass (19th–20th centuries AD).

### 5.2.2.4 Outliers

USTRA-02 does not have any indication of recycling or intentional addition of colorants. Iron oxide content of 1.56 wt% and lack of decolorant (MnO=0.33 wt%), along with the furnace conditions appears to be sufficient to color the glass emerald green. USPAR-03 is a blue colored glass that has a similar amount of trace elements regarding the use of colorant and recycling as USPAR-10 from Cluster 2.

## 6 Conclusions

The glass samples examined are very fragmented and consequently, in many cases, it was not possible to define them typologically. In addition, most of the glass samples showed signs of severe alteration with depletion and enrichment of some major elements; this is the reason for using rubidium and strontium values as proxies as they proved to be useful in clustering the fragments.

Combining the results of geochemical and typological analyses, most of Ustica glass fragments have been attributed to compositional groups. Furthermore, knowing that the island of Ustica has been inhabited discontinuously, with centuries of intense population and centuries of total abandonment, it was also possible to verify the compatibility between the chemical data with the epoch of each glass artifact manufacturing and the time of their probable use.

The intense occupation of the island during the 4th–6th century AD is attested by fragments of Cluster 1 that are associated with the Roman Levantine production (Table 2, Figure 5). In this group, a problem is raised by the fragments USPAR-01 and 11 which perfectly juxtapose, representing two pieces of the same object, a unguentarium or an oil lamp with a pointed base (Table 1). Despite this, they show slight chemical differences in the major elements, and more marked in the concentrations of Pb and normalized REE. This discrepancy could be explained both in terms of compositional heterogeneity and the variable degree of alteration, or the possibility that these two pieces are parts of two different vessels of the same type. The latter would, consequently, require further investigation of the restoration procedures and carrying out a study that would include sampling several fragments of the same vessel with a representative number of specimens. Possibly, the first step would be performing more analyses on USPAR-01 and 11 as the question of them belonging to the same vessel remains unresolved.

The Early Byzantine period (6th century AD) is represented by high-alumina plant ash glass of Cluster 2, whose origins can potentially be found in Asia. Unfortunately, all these fragments are not referable to a specific typology because of the absence of diagnostic elements in their bodies.

Following an occupational gap, during the last colonization of Ustica in 18th-century HLLA glass represented by the outlier USPAR-06 was introduced, while in the 19th-century modern synthetic soda glass starts to dominate the glass assemblage of the island.

Summing up, all the archaeological and chemical data combined evidence of the discontinuous settlement of the island and the import of the glass materials.

# References

Abdalla, H. M., Helba, H. A., & Mohamed, F. H. (1998). Chemistry of columbite-tantalite minerals in rare metal granitoids, Eastern Desert, Egypt. *Mineralogical Magazine, 62*(6), 821–836. https://doi.org/10.1180/002646198548197

Adlington, L. W., Freestone, I. C., & Teed, N. (2015). *Analysis of medieval stained glass by handheld pXRF*. Poster presented at TECHNART 2015: Non-destructive and microanalytical techniques in art and cultural heritage, Catania, 27-30 April 2015.

Adlington, L. W., & Freestone, I. C. (2017). Using handheld pXRF to study medieval stained glass: A methodology using trace elements. *MRS Advances, 2*(33-34), 1785–1800. https://doi.org/10.1557/adv.2017.233

Ailara, V. (2015). Beauty in Hystory. In Ailara, V., de Vita, S. Foresta Martin, F., & Nicoletti, T. (Eds.), *L'Isola di Ustica. Il racconto della Bellezza attraverso le parole, le immagini e le note musicali*. Palermo: Regione siciliana, Assessorato dei beni culturali e dell'identità siciliana.

Angelini, I., Gratuze, B., & Artioli, G. (2019). *Glass and other vitreous materials through history* (Vol. 20). EMU Notes in Mineralogy. https://doi.org/10.1180/EMU-notes.20.3

Arletti, R., Vezzalini, G., Biaggio Simona, S., & Maselli Scotti, F. (2008). Archaeometrical studies of Roman imperial age glass from Canton Ticino. *Archaeometry, 50*(4), 606–626. https://doi.org/10.1111/j.1475-4754.2007.00362.x

Auriemma, R. (2000). Le anfore del relitto di Grado e il loro contenuto. *Mélanges de l'école française de Rome, 112*(1), 27–51.

Barbera, G., Barone, G., Crupi, V., Longo, F., Majolino, D., Mazzoleni, P., . . . Venuti, V. (2012). Study of Late Roman and Byzantine glass by the combined use of analytical techniques. *Journal of Non-Crystalline Solids, 358*(12-13), 1554–1561. https://doi.org/10.1016/j.jnoncrysol.2012.04.013

Barca, D., De Francesco, A. M., Crisci, G. M., & Tozzi, C. (2008). Provenance of obsidian artifacts from site of Colle Cera, Italy, by LA-ICP-MS method. *Periodico di Mineralogia, 77*, 41–52.

Barca, D., Abate, M., Crisci, G. M., & De Presbiteris, D. (2009). Post-Medieval glass from the castle of Cosenza, Italy: Chemical characterization by LA-ICP-MS and SEM-EDS. *Periodico di Mineralogia*, *78*(2), 49–64. https://doi.org/10.2451/2009PM0008

Barca, D., Basso, E., Bersani, D., Galli, G., Invernizzi, C., La Russa, M.F., . . . Ruffolo, S. A. (2016). Vitreous tesserae from the calidarium mosaics of the Villa dei Quintili, Rome. Chemical composition and production technology. *Microchemical Journal*, *124*, 726–735. https://doi.org/10.1016/j.microc.2015.10.037

Barca, D., Fiorenza, E., D'Andrea, M., Le Pera, E., Musella, M., Sudano, F., & Taliano Grasso, A. (2019). Chemical and Petrographic Characterization of Stone and Glass Tesserae in the Nereid and Geometric Mosaics from the S. Aloe Quarter in Vibo Valentia–Calabria, Italy. *Minerals*, *9*(12), 729. https://doi.org/10.3390/min9120729

Basile, B., Carreras Rossel, T., Greco, C., & Spanò Giammellaro A. (2004*). Glassway. Il vetro: fragilità attraverso il tempo*. Soprintendenza ai Beni Culturali e Ambientali di Ragusa.

Basso, E., Riccardi, M. P., Messiga, B., Mendera, M., Gimeno, D., Garcia-Valles, M., . . . Tarozzi, C. (2009). Composition of the base glass used to realize the stained glass windows by Duccio di Buoninsegna (Siena Cathedral, 1288-1289 AD): A geochemical approach. *Materials Characterization, 60*(12), 1545–1554. https://doi.org/10.1016/j.matchar.2009.09.005

Brems, D., Degryse, P., Hasendoncks, F., Gimeno, D., Silvestri, A., Vassilieva, E., . . . Honings, J. (2012). Western Mediterranean sand deposits as a raw material for Roman glass production. *Journal of Archaeological Science, 39*(9), 2897–2907. https://doi.org/10.1016/j.jas.2012.03.009

Brill, R. H. (1962). A note on the scientist's definition of glass. *Journal of Glass Studies, 4*, 127–138.

Brill, R. H. (1999a). Chemical Analyses of Early Glasses (Vol. 1. The Catalogue). Corning, N.Y.: Corning Museum of Glass.

Brill, R. H. (1999b). Chemical Analyses of Early Glasses (Vol. 2. The Tables). Corning, N.Y.: Corning Museum of Glass.

Cagno, S., Mendera, M., Jeffries, T., & Janssens, K. (2010). Raw materials for medieval to post-medieval Tuscan glassmaking: New insight from LA-ICP-MS analyses. *Journal of Archaeological Science, 37*(12), 3030–3036. https://doi.org/10.1016/j.jas.2010.06.030

Carter, A. K. (2016). The Production and Exchange of Glass and Stone Beads in Southeast Asia from 500 BCE to the early second millennium CE: An assessment of the work of Peter Francis in light of recent research. *Archaeological Research in Asia, 6*, 16–29. https://doi.org/10.1016/j.ara.2016.02.004

Coutinho, I., Gratuze, B., Alves, L. C., Medici, T., & Vilarigues, M. (2017). Wine Bottles From Lisbon: Archaeometric Studies Of Two Archaeological Sites Dated From The 17th To The 19th Century. *Archaeometry, 59*(5), 852–873. https://doi.org/10.1111/arcm.12283

Davison, S. (2003). *Conservation and Restoration of Glass*. Oxford: Butterworth-Heinemann.

De Bardi, M., Wiesinger, R., & Schreiner, M. (2013). Leaching studies of potash-lime-silica glass with medieval composition by IRRAS. *Journal of Non-Crystalline Solids, 360*(1), 57–63. https://doi.org/10.1016/j.jnoncrysol.2012.06.035

Degryse, P. (Ed.). (2014). *Glass making in the Greco-Roman world: results of the ARCHGLASS project* (Studies in Archaeological Sciences, Vol. 4). Leuven University Press. https://doi.org/10.26530/OAPEN_513796

Degryse, P., Scott, R. B., & Brems, D. (2014). The archaeometry of ancient glassmaking: reconstructing ancient technology and the trade of raw materials. *Perspective. Actualité en histoire de l'art*, *2*, 224–238. https://doi.org/10.4000/perspective.5617

de Vita, S., Laurenzi, M. A., Orsi, G., & Voltaggio, M. (1998). Application of 40Ar/39Ar and 230Th dating methods to the chronostratigraphy of Quaternary basaltic volcanic areas: The Ustica island case history. *Quaternary International, 47-48*, 117–127. https://doi.org/10.1016/S1040-6182(97)00077-3

de Vita, S., & Foresta Martin, F. (2017). The palaeogeographic setting and the local environmental impact of the 130 ka Falconiera tuff-cone eruption (Ustica island, Italy). *Annals of Geophysics, 60*(2), S0224. https://doi.org/10.4401/ag-7113

Dungworth, D. (2017). A tale of two industries: The manufacture of bottle and window glass in England from the 17th to the 20th centuries. In: Coutinho, I., Palomar, T., Coentro, S., Machado, A., & Vilarigues, M. (Eds.), *Proceedings of the 5th GLASSAC International Conference. 2017 FTC Nova* (pp. 9–10). NOVA.FCT Editorial. Retrieved from https://eventos.fct.unl.pt/glassac2017/files/actas_glassac.pdf

Dungworth, D., Bower, H., Gilchrist, A., & Wilkes, R. (2010). The West Window Beverley Minster Beverley, East Yorkshire. Chemical Analysis of the Window Glass and Paint. *Research Department Report Series*, *25*,1–24.

Dussubieux, L., Gratuze, B., & Blet-Lemarquand, M. (2010). Mineral soda alumina glass: Occurence and meaning. *Journal of Archaeological Science, 37*(7), 1646–1655. https://doi.org/10.1016/j.jas.2010.01.025

Dussubieux, L., & Gratuze, B. (2013). Glass in South Asia. *Modern Methods for Analysing Archaeological and Historical Glass*, *1*, 399-413.

Farges, F., Etcheverry, M.-P., Scheidegger, A., & Grolimund, D. (2006). Speciation and weathering of copper in "copper red ruby" medieval flashed glasses from the Tours cathedral (XIII century). *Applied Geochemistry*, *21*(10), 1715–1731. https://doi.org/10.1016/j.apgeochem.2006.07.008

Foresta Martin F. (2014). *Ustica prima dell'Uomo*. Ustica: Centro Studi e Documentazione Isola di Ustica.

Foresta Martin, F., Di Piazza, A., D'Oriano, C., Carapezza, M. L., Paonita, A., Rotolo, S. G., & Sagnotti, L. (2017). New insights into the provenance of the obsidian fragments of the island of Ustica (Palermo, Sicily). *Archaeometry, 59*(3), 435–454. https://doi.org/10.1111/arcm.12270

Foresta Martin, F., & La Monica, M. (2019). The Black Gold that came from the sea. A review of obsidian studies at the island of Ustica, Italy. *Annals of Geophysics, 62*(1), 1–15. https://doi.org/10.4401/ag-7686

Freestone, I. C. (2001). Post-depositional changes in archaeological ceramics and glasses. In D. R. Brothwell & A. M. Pollard (Eds.), *Handbook of archaeological sciences* (pp. 615–625). Wiley.

Freestone, I. (2004). The Provenance of Ancient Glass through Compositional Analysis. *MRS Proceedings, 852*, OO8.1. doi:10.1557/PROC-852-OO8.1

Freestone, I. C., Gorin-Rosen, Y., & Hughes, M. J. (2000). Primary glass from Israel and the production of glass in late antiquity and the early Islamic period. *MOM Éditions, 33*(1), 65–83.

Freestone, I. C., Hughes, M. J., & Stapleton, C. P. (2008). The composition and production of Anglo-Saxon glass. In S. Marzintik (Ed.), *Catalogue of Anglo-Saxon Glass in the British Museum* (pp. 29–46). London: The British Museum.

Freestone, I. C., Wolf, S., & Thirlwall, M. (2009). Isotopic composition of glass from the Levant and south-eastern Mediterranean Region. In Degryse, P., Henderson, J., & Hodgins, G. (Eds.), *Isotopes in vitreous materials* (Studies in archaeological sciences, Vol. 1, pp. 31–52). Leuven University Press.

Freestone, I., Degryse, P., Lankton, J., Gratuze, B., & Schneider, J. (2018). HIMT, glass composition and commodity branding in the primary glass industry. In Rosenow D., Phelps M., Meek A., & Freestone I. (Eds.), *Things that Travelled: Mediterranean Glass in the First Millennium AD* (pp. 159–190). London: UCL Press. https://doi.org/10.2307/j.ctt21c4tb3.14

Friedrich, K. T. & Degryse, P. (2019). Soil vs. glass: an integrated approach towards thecharacterization of soil as a burial environment forthe glassware of Cucagna Castle (Friuli, Italy*). STAR: Science & Technology of Archaeological Research*. https://doi.org/10.1080/20548923.2019.1688492

Fryer, B. J., Jackson, S. E., & Longerich, H. P. (1995). The design, operation and role of the laser-ablation microprobe coupled with an inductively coupled plasma-mass spectrometer (LAM-ICP-MS) in the Earth sciences. *Canadian Mineralogist, 33*, 303–312.

Gao, S., Liu, X., Yuan, H., Hattendorf, B., Gunther, D., Chen, L., & Hu, S. (2002). Determination of forty-two major and trace elements in USGS and NIST SRM glasses by laser ablation-inductively coupled plasma mass spectrometry. *Geostandards Newsletter: The Journal of Geostandards and Geoanalysis, 26*(2), 181–196. https://doi.org/10.1111/j.1751-908X.2002.tb00886.x

Genga, A., Siciliano, M., Famà, L., Filippo, E., Siciliano, T., Mangone, A., . . . Laganara, C. (2008). Characterization of surface layers formed under natural environmental conditions on medieval glass from Siponto (Southern Italy). *Materials Chemistry and Physics, 111*(2–3), 480–485. https://doi.org/10.1016/j.matchemphys.2008.04.057

Gratuze, B., & Barrandon, J. N. (1990). Islamic glass weights and stamps: Analysis using nuclear techniques. *Archaeometry, 32*(2), 155–162. https://doi.org/10.1111/j.1475-4754.1990.tb00462.x

Gratuze, B., & Janssens, K. (2004). Provenance analysis of glass artefacts. In K. H. Janssens & R. Grieken (Eds.), *Wilson & Wilson's Comprehensive Analytical Chemistry*. Elsevier.

Gratuze, B., Soulier, I., Barrandon, J.-N., & Foy, D. (1995). The origin of cobalt blue pigments in French glass from the thirteenth to the eighteenth centuries. In D. R. Hook & D. R. M. Gaimster (Eds.), *Trade and Discovery: The Scientific Study of Artefacts from Post-Medieval Europe and Beyond* (pp. 123–133). London: Bristish Museum Press.

Gratuze, B., Soulier, I., Barrandon, J. N., & Roy, D. (1992). De l'origine du cobalt dans les verres. *Revue d'Archeometrie, 16*(1), 97–108. Retrieved from http://www.persee.fr/web/revues/home/prescript/article/arsci_0399-1237_1992_num_16_1_895 https://doi.org/10.3406/arsci.1992.895

Gratuze, B. (2013). Provenance analysis of glass artefacts. In K. Janssens (Ed.), *Modern methods for analysing archaeological and historical glass* (pp. 311–343). Wiley & Sons, Ltd https://doi.org/10.1002/9781118314234.ch14

Gueriau, P., Jauvion, C., & Mocuta, C. (2018). Show me your yttrium, and I will tell you who you are: Implications for fossil imaging. *Palaeontology, 61*(6), 981–990. https://doi.org/10.1111/pala.12377

Gunther, D., & Heinrich, C. A. (1999). Enhanced sensitivity in laser ablation-ICP mass spectrometry using helium-argon mixtures as aerosol carrier. *Journal of Analytical Atomic Spectrometry, 14*(9), 1363–1368. https://doi.org/10.1039/A901648A

Hellemans, K., Cagno, S., Bogana, L., Janssens, K., & Mendera, M. (2019). LA-ICP-MS labels early medieval Tuscan finds from Siena and Donoratico as late natron glass. *Journal of Archaeological Science, Reports, 23*, 844–853. https://doi.org/10.1016/j.jasrep.2018.12.002

Isings, C. (1957). *Roman glass from dated finds* (Vol. 2). JB Wolters.

Janssens, K. (2013). *Modern Methods for Analysing Archaeological and Historical Glass*. John Wiley & Sons. https://doi.org/10.1002/9781118314234

Križanac, M. (2016). Early Byzantine Glass in the Territory of Serbia and Kosovo. *Journal of Glass Studies, 58*, 87–103.

Lifshin, E. (2006). Electron Microprobe Analysis. In R. W. Cahn, P. Haasen, & E.J. Kramer (Eds.), *Materials Science and Technology* (pp. 352–521). Weinheim, Germany: Wiley-VCH Verlag GmbH & Co. KGaA. https://doi.org/10.1002/9783527603978.mst0025

Mannino, G., & Ailara, V. (2016). *Carta archeologica di Ustica*. Ustica : Centro studi e documentazione isola di Ustica.

Mirti, P., Casoli, A., & Appolonia, L. (1993). Scientific analysis of Roman glass from Augusta Praetoria. *Archaeometry, 35*(2), 225–240. https://doi.org/10.1111/j.1475-4754.1993.tb01037.x

Mirti, P., Lepora, A., & Sagui, L. (2000). Scientific analysis of seventh-century glass fragments from the Crypta Balbi in Rome. *Archaeometry, 42*(2), 359–374. https://doi.org/10.1111/j.1475-4754.2000.tb00887.x

Nenna, M. D. (Ed.). (2000). *La route du verre: ateliers primaires et secondaires du second millénaire av. J.-C. au Moyen Age*. Lyon, Maison de l'Orient et de la Méditerranée-Jean Pouilloux.

Nenna, M. D. (2015). *Primary glass workshops in Graeco-Roman Egypt. Glass of the Roman Empire*. Oxford: Oxbow Books.

Orlando, A., Olmi, F., Vaggelli, G., & Bacci, M. (1996). Mediaeval Stained Glasses of Pisa Cathedral (Italy): Their Composition and Alteration Products. *Analyst, 121*(4), 553–558. https://doi.org/10.1039/an9962100553

Ortega-Feliu, I., Gómez-Tubío, B., Respaldiza, M. A., & Capel, F. (2011). Red layered medieval stained glass window characterization by means of micro-PIXE technique. *Nuclear Instruments & Methods in Physics Research. Section B, Beam Interactions with Materials and Atoms, 269*(20), 2378–2382. https://doi.org/10.1016/j.nimb.2011.02.023

Palomar, T. (2018). Chemical composition and alteration processes of glasses from the Cathedral of León (Spain). *Boletín de la Sociedad Española de Cerámica y Vidrio, 57*(3), 101–111. https://doi.org/10.1016/j.bsecv.2017.10.001

Pearce, N. J. G., Perkins, W. T., Westgate, J. A., Gorton, M. T., Jackson, S. E., Neal, C. R., & Chenery, S. P. (1997). A compilation of new and published major and trace element data for NIST SRM 610 and SRM 612 glass reference materials. *Geostandards Newsletter, 21*(1), 115–144. https://doi.org/10.1111/j.1751-908X.1997.tb00538.x

Picon, M., & Vichy, M. (2003). D'Orient en Occident: l'origine du verre à l'époque romaine et durant le haut Moyen Âge. In Foy, D., & Marie-Dominique Nenna, M.-D. (Eds.), *Échanges et commerce du verre dans le monde antique (Actes du colloque de l'AFAV, Aix-en-Provence et Marseille, 7-9 juin 2001)* (pp. 17–31). Anvers.

Pion, C., & Gratuze, B. (2016). Indo-Pacific glass beads from the Indian subcontinent in Early Merovingian graves (5th–6th century AD). *Archaeological Research in Asia,* (6) 51–64. https://doi.org/10.1016/j.ara.2016.02.005

Pliny the Elder. (1962). *Natural history* (Rackham, H., & Jones, W. H. S., Trans.). London : William Heinemann.

Pollard, A. M., & Heron, C. (2008). *Archaeological Chemistry*. Cambridge: Royal Society of Chemistry.

Posedi, I. (2016). *Characterization of medieval glass artefacts from Miranduolo site, Chiusdino, Italy*. Master's thesis, Universidade de Évora.

Posedi, I. (2020). *Thirteenth-century Lincoln Cathedral stained-glasses: physico-chemical analyses of the Dean's Eye rose window and south lancet window SG32*. Unpublished PhD thesis. University of Lincoln.

Posedi, I., Kertész, Z., Barrulas, P., Fronza, V., Schiavon, N., & Mirão, J. (2019). Medieval Tuscan glasses from Miranduolo, Italy: A multi-disciplinary study. *Journal of Archaeological Science, Reports, 26*, 101878. https://doi.org/10.1016/j.jasrep.2019.101878

Posedi, I., Schiavon, N., Mirão, J., & Fronza, V. (2016). Archaeovitreological Study by VP-SEM-EDS of Glass Fragments (1250–1350 AD) from Miranduolo, Chiusdino, Italy. Paper presented at *50th Meeting of SPMicros – Microscopy and Microanalysis in Materials and Life Sciences*, Porto, 29-30 June 2016.

Poulain, D., Scuiller, C. & Gratuze, B. (2013). La parure en verre et en ambre de la nécropole mérovingienne de Saint-Laurent-des-Hommes (Dordogne). *Bulletin de l'Association Française de l'Archéologie du Verre*, 72–79.

Rapp, G. (2009). *Archaeomineralogy*. Heidelberg: Springer-Verlag. https://doi.org/10.1007/978-3-540-78594-1

Rehren, T., & Freestone, I. C. (2015). Ancient glass: From kaleidoscope to crystal ball. *Journal of Archaeological Science, 56*, 233–241. https://doi.org/10.1016/j.jas.2015.02.021

Sayre, E. V., & Smith, R. W. (1961). Compositional categories of ancient glass. *Science, 133*(3467), 1824–1826. https://doi.org/10.1126/science.133.3467.1824

Schalm, O., Janssens, K., Wouters, H., & Caluwé, D. (2007). Composition of 12–18th century window glass in Belgium: Non-figurative windows in secular buildings and stained-glass windows in religious buildings. *Spectrochimica Acta. Part B, Atomic Spectroscopy, 62*(6-7), 663–668. https://doi.org/10.1016/j.sab.2007.03.006

Schibille, N., & Freestone, I. C. (2013). Composition, production and procurement of glass at San Vincenzo Al Volturno: An early Medieval monastic complex in Southern Italy. *PLoS One, 8*(10), e76479. https://doi.org/10.1371/journal.pone.0076479

Scott Ercit, T. (1994). The geochemistry and crystal chemistry of columbite-group minerals from granitic pegmatites, southwestern Grenville province, Canadian shield. *Canadian Mineralogist, 32*, 421–438.

Shackelford, J. F., & Doremus, R. H. (Eds.). (2008). *Ceramic and Glass Materials: Structure, Properties and Processing*. Boston: Springer https://doi.org/10.1007/978-0-387-73362-3

Silvestri, A., Molin, G., & Salviulo, G. (2005). Archaeological glass alteration products in marine and land-based environments: Morphological, chemical and microtextural characterization. *Journal of Non-Crystalline Solids, 351*(16-17), 1338–1349. https://doi.org/10.1016/j.jnoncrysol.2005.03.013

Sode, T., Gratuze, B., & Lankton, J. (2017). Red and orange high-alumina glass beads in 7th and 8th century Scandinavia: Evidence for long distance trade and local fabrication. In Wolf, S. & de Pury-Gysel, A. (Eds), *Annales du 20e congrès de l'Association Internationale pour l'Histoire du Verre* (pp. 326–333). Romont: AIHV - Association Internationale pour l'Histoire du Verre

Spatafora, F., & Mannino, G. (Ed.). (2008). Ustica, Brief Guide. Palermo: Beni Culturali e Ambientali.

Swan, C. M., Rehren, T., Dussubieux, L., & Eger, A. A. (2018). High-boron and High-alumina Middle Byzantine (10th-12th Century ce) Glass Bracelets: A Western Anatolian Glass Industry : Middle Byzantine glass bracelets. *Archaeometry, 60*(2), 207–232. https://doi.org/10.1111/arcm.12314

Then-Obłuska, J., & Dussubieux, L. (2016). Glass bead trade in the Early Roman and Mamluk Quseir ports—A view from the Oriental Institute Museum assemblage. *Archaeological Research in Asia, 6*, 81–103. https://doi.org/10.1016/j.ara.2016.02.008

Then-Obłuska, J., Wagner, B., & Kepa-Linowska, L. (2019). Dare to Gaze upon Her Face: An Interdisciplinary Analysis of Mosaic Face Beads from Meroe. *Journal of Glass Studies, 61*, 39.

Tite, M., Shortland, A., & Paynter, S. (2002). The beginnings of vitreous materials in the Near East and Egypt. *Accounts of Chemical Research, 35*(8), 585–593. https://doi.org/10.1021/ar000204k

Toniolo, A. (2005). Musealizzazione del relitto di epoca imperiale romana Iulia Felix di grado (Italia) nel nuovo museo di archeologia subacquea di grado: il relitto e il suo carico. In *De la excavación al público: procesos de decisión y creación de nuevos recursos* (pp. 161-164). Zaragoza: Ayuntamiento de Zaragoza, Área de Cultura y Turismo, Servicio de Cultura

Trouth, P. (2017). Murano: removing arsenic brings benefits to health and the environment. *ECHA Newsletter*, Available from https://newsletter.echa.europa.eu/home/-/newsletter/entry/murano-removing-arsenic-brings-benefits-to-health-and-the-environment

Tykot, R. H. (1995). Appendix I: obsidian provenance. In R.R. Holloway & S.S. Lukesh (Eds.), *Ustica I. The Results of the Excavations of the Regione Siciliana Soprintendenza ai Beni Culturali ed Ambientali Provincia di Palermo in Collaboration with Brown University in 1990 and 1991* (pp. 87–90). Providence, R.I.: Center for Old World Archaeology and Art, Brown University.

van Achterberg, E., Ryan, C. G., Jackson, S. E., & Griffin, W. L. (2001). Data reduction software for LA-ICPMS: appendix. In P. J. Sylvester (Ed.), *Laser Ablation-ICP-Mass Spectrometry in the Earth Sciences: Principles and Applications. Mineralogical Association of Canada (MAC)* (Vol. 29, pp. 239–243). Short Course Series.

Verità, M. & Zecchin, S. (2016). Raw materials and glassmaking technology in nineteenth-century Murano glassworks. In Barovier Mentasti, R., &Tonini, C. (Eds.), *Study Days on Venetian Glass. The Birth of the Great Museum: the Glassworks Collections Between the Renaissance and the Revival.* (pp. 45–56). Venezia: Istituto Veneto di Scienze, Lettere ed Arti.

Wedepohl, K. H., Simon, K., & Kronz, A. (2011). Data on 61 chemical elements for the characterization of three major glass compositions in late antiquity and the middle ages. *Archaeometry, 53*(1), 81–102. https://doi.org/10.1111/j.1475-4754.2010.00536.x

Wedepohl, K. H. (1995). The composition of the continental crust. *Geochimica et Cosmochimica Acta, 59*(7), 1217–1232. https://doi.org/10.1016/0016-7037(95)00038-2

Wood, M., Panighello, S., Orsega, E. F., Robertshaw, P., van Elteren, J. T., Crowther, A., . . . Boivin, N. (2017). Zanzibar and Indian Ocean trade in the first millennium CE: The glass bead evidence. *Archaeological and Anthropological Sciences, 9*(5), 879–901. https://doi.org/10.1007/s12520-015-0310-z